ISSN 1949-8470 (online)

World Journal of *Radiology*

World J Radiol 2021 October 28; 13(10): 314-353

Published by Baishideng Publishing Group Inc

World Journal of
Radiology

Monthly Volume 13 Number 10 October 28, 2021

Contents

ABOUT COVER

Editorial Board Member of *World Journal of Radiology*, Ozum Tuncyurek, MD, EDIR, Associate Professor, Chief, Department of Radiology, Faculty of Medicine, Near East University, Nicosia 99138, Turkey. ozum.tuncyurek@neu.edu.tr

AIMS AND SCOPE

The primary aim of *World Journal of Radiology* (*WJR*, *World J Radiol*) is to provide scholars and readers from various fields of radiology with a platform to publish high-quality basic and clinical research articles and communicate their research findings online.

WJR mainly publishes articles reporting research results and findings obtained in the field of radiology and covering a wide range of topics including state of the art information on cardiopulmonary imaging, gastrointestinal imaging, genitourinary imaging, musculoskeletal imaging, neuroradiology/head and neck imaging, nuclear medicine and molecular imaging, pediatric imaging, vascular and interventional radiology, and women's imaging.

INDEXING/ABSTRACTING

The *WJR* is now abstracted and indexed in Emerging Sources Citation Index (Web of Science), PubMed, PubMed Central, China National Knowledge Infrastructure (CNKI), China Science and Technology Journal Database (CSTJ), and Superstar Journals Database. The 2021 edition of Journal Citation Reports® cites the 2020 Journal Citation Indicator (JCI) for *WJR* as 0.51.

RESPONSIBLE EDITORS FOR THIS ISSUE

Production Editor: *Ji-Hong Liu*; **Production Department Director:** *Yu-Jie Ma*; **Editorial Office Director:** *Jia-Ping Yan*.

NAME OF JOURNAL
World Journal of Radiology

ISSN
ISSN 1949-8470 (online)

LAUNCH DATE
January 31, 2009

FREQUENCY
Monthly

EDITORS-IN-CHIEF
Venkatesh Mani

EDITORIAL BOARD MEMBERS
https://www.wjgnet.com/1949-8470/editorialboard.htm

PUBLICATION DATE
October 28, 2021

INSTRUCTIONS TO AUTHORS
https://www.wjgnet.com/bpg/gerinfo/204

GUIDELINES FOR ETHICS DOCUMENTS
https://www.wjgnet.com/bpg/GerInfo/287

GUIDELINES FOR NON-NATIVE SPEAKERS OF ENGLISH
https://www.wjgnet.com/bpg/gerinfo/240

PUBLICATION ETHICS
https://www.wjgnet.com/bpg/GerInfo/288

PUBLICATION MISCONDUCT
https://www.wjgnet.com/bpg/gerinfo/208

ARTICLE PROCESSING CHARGE
https://www.wjgnet.com/bpg/gerinfo/242

STEPS FOR SUBMITTING MANUSCRIPTS
https://www.wjgnet.com/bpg/GerInfo/239

ONLINE SUBMISSION
https://www.f6publishing.com

World Journal of Radiology

Submit a Manuscript: https://www.f6publishing.com

World J Radiol 2021 October 28; 13(10): 314-326

DOI: 10.4329/wjr.v13.i10.314

ISSN 1949-8470 (online)

FRONTIER

Current trends and perspectives in interventional radiology for gastrointestinal cancers

Elisa Reitano, Nicola de'Angelis, Giorgio Bianchi, Letizia Laera, Stavros Spiliopoulos, Roberto Calbi, Riccardo Memeo, Riccardo Inchingolo

ORCID number: Elisa Reitano 0000-0002-4286-8866; Nicola de'Angelis 0000-0002-1211-4916; Giorgio Bianchi 0000-0003-0245-3460; Letizia Laera 0000-0003-2183-8817; Stavros Spiliopoulos 0000-0003-1860-0568; Roberto Calbi 0000-0003-0934-8890; Riccardo Memeo 0000-0002-1668-932X; Riccardo Inchingolo 0000-0002-0253-5936.

Author contributions: Reitano E contributed to the manuscript concept, the study design, literature search, data interpretation, and article drafting; de'Angelis N, Bianchi G, Laera L, Spiliopoluos S, Calbi R and Memeo R contributed to the concept, the study design, data analysis, data interpretation, and manuscript critical revision; Inchingolo R contributed to the concept, the study design, data analysis, data interpretation, article drafting and manuscript critical revision; all authors read and approve the final version of the manuscript.

Conflict-of-interest statement: All the authors are aware of the content of the manuscript and have no conflict of interest.

Elisa Reitano, Division of General Surgery, Department of Translational Medicine, University of Eastern Piedmont, Novara 28100, Italy

Nicola de'Angelis, Giorgio Bianchi, Unit of Minimally Invasive and Robotic Digestive Surgery, "F. Miulli" General Regional Hospital, Acquaviva delle Fonti 70021, Italy

Letizia Laera, Department of Oncology, "F. Miulli" General Regional Hospital, Acquaviva delle Fonti 70021, Italy

Stavros Spiliopoulos, 2nd Department of Radiology, School of Medicine, National and Kapodistrian University of Athens, Athens 12461, Greece

Roberto Calbi, Department of Radiology, "F. Miulli" General Regional Hospital, Acquaviva delle Fonti 70124, Italy

Riccardo Memeo, Unit of Hepato-Pancreatic-Biliary Surgery, "F. Miulli" General Regional Hospital, Acquaviva delle Fonti 70021, Italy

Riccardo Inchingolo, Interventional Radiology Unit, "F. Miulli" General Regional Hospital, Acquaviva delle Fonti 70021, Italy

Corresponding author: Riccardo Inchingolo, MD, Chief Doctor, Director, Interventional Radiology Unit, "F. Miulli" General Regional Hospital, Strada per Santeramo, Acquaviva delle Fonti 70021, Italy. riccardoin@hotmail.it

Abstract

Gastrointestinal (GI) cancers often require a multidisciplinary approach involving surgeons, endoscopists, oncologists, and interventional radiologists to diagnose and treat primitive cancers, metastases, and related complications. In this context, interventional radiology (IR) represents a useful minimally-invasive tool allowing to reach lesions that are not easily approachable with other techniques. In the last years, through the development of new devices, IR has become increasingly relevant in the context of a more comprehensive management of the oncologic patient. Arterial embolization, ablative techniques, and gene therapy represent useful and innovative IR tools in GI cancer treatment. Moreover, IR can be useful for the management of GI cancer-related complications, such as bleeding, abscesses, GI obstructions, and neurological pain. The aim of this study is to show the principal IR techniques for the diagnosis and treatment of GI cancers and

Manuscript source: Invited manuscript

Specialty type: Radiology, nuclear medicine and medical imaging

Country/Territory of origin: Italy

Peer-review report's scientific quality classification

Grade A (Excellent): 0
Grade B (Very good): 0
Grade C (Good): C, C, C, C
Grade D (Fair): 0
Grade E (Poor): 0

Received: March 28, 2021
Peer-review started: March 28, 2021
First decision: June 3, 2021
Revised: June 12, 2021
Accepted: October 9, 2021
Article in press: October 9, 2021
Published online: October 28, 2021

P-Reviewer: Kamada Y, Kanat O, Vasani J
S-Editor: Fan JR
L-Editor: A
P-Editor: Fan JR

related complications, as well as to describe the future perspectives of IR in this oncologic field.

Key Words: Interventional radiology; Radiology; Colorectal cancer; Gastric cancer; Malignancy; Embolization

Core Tip: Interventional radiology is a minimally-invasive tool for the diagnosis and treatment of different gastrointestinal cancers, representing a useful alternative to more invasive approaches such as surgery and endoscopy. Hereby, we describe the different radiological techniques for the diagnosis and treatment of gastrointestinal cancers and related complications, underlining the role of this specialty in cancer patient's care.

Citation: Reitano E, de'Angelis N, Bianchi G, Laera L, Spiliopoulos S, Calbi R, Memeo R, Inchingolo R. Current trends and perspectives in interventional radiology for gastrointestinal cancers. *World J Radiol* 2021; 13(10): 314-326
URL: https://www.wjgnet.com/1949-8470/full/v13/i10/314.htm
DOI: https://dx.doi.org/10.4329/wjr.v13.i10.314

INTRODUCTION

Gastrointestinal (GI) cancers are currently among the five most common cancers worldwide for both men and women[1]. According to the GLOBOCAN 2018, colon cancer and gastric cancer represents respectively the 3rd and 5th most common cancers [2,3]. Some GI, such as the pancreatic cancer (PC), are rarer but burdened by a high mortality rate[4]. PC represents the thirteen most common cancer and the seventh most common cause of cancer-related death[4]. The incidence of GI cancer shows significant geographical variations, with colorectal cancer incidence higher in Western Countries and North America[3,5], whereas gastric cancer incidence is higher in Asia and Africa[2]. These geographical differences are mainly linked to environmental and lifestyle factors such as nutritional habits, alcohol intake, genetics, and obesity[2,5].

Nowadays, the "gold standard" management of cancers involves a multi-specialist staff consisting of oncologists, surgeons, endoscopists, and radiologists to provide a multi-disciplinary diagnostic and treatment approach to the oncologic patient.

Interventional radiology (IR) is getting a key role in oncologic patients' cares, being an essential tool in both the initial diagnosis and the subsequent treatment, as well as in the management of the related complications[6]. IR provides adequate diagnostic samples through a minimally invasive access, which can be obtained under imagine guidance by percutaneous and needle aspiration[7]. Therapeutic applications of IR in oncology are mainly focused on local cancer treatment, including radiofrequency (RF) ablation or trans-arterial chemoembolization (TACE)[8]. Cancers complications, such as pain, bleeding, organ obstructions, or venous thrombosis can also be managed by IR, with the eventual placement of gastrostomy or jejunostomy in selected patients[9,10].

This article aims to analyse the current roles of IR in GI cancer management and provide an extensive overview of the current literature on the topic. In this article, only cancers located in the GI tract (from the esophagus to the colon) will be considered. Liver, pancreas, and biliary tract will not be taken into account, as they should require a separate discussion.

IR IN THE DIAGNOSIS OF GI CANCERS

The adequate treatment of GI cancers depends on a timely definitive diagnosis and the staging of the disease[11]. Imaging techniques improved the assessment and staging of cancers, but the histological analysis represents the gold standard for the definitive diagnosis of this disease. Biopsies samples are required to assess the biomarker status of different solid GI cancers and should be performed not only for the initial diagnosis but at multiple end-points, to detect the cancer progression, predict the prognosis and guide the next-line therapy[12]. The improvement of the histological and cytological analysis, especially in the field of immunochemical examination, enables the identification of the primary tumor site and predicts the sensitivity to chemotherapeutic drugs[13].

Minimally invasive techniques have a prominent role in this contest. Endoscopy currently represents the first-level procedure for the histological diagnosis of GI cancers. However, lesions located within the submucosa or subserosa (such as lymphoma or gastrointestinal stromal tumours), may be difficult to diagnose with this approach[14]. Cancers located in the small bowel or colon could be not always reachable by the endoscope, due to their location or to stenosis of the lumen[14]. In this case, biopsies can obtain by interventional radiologists through direct visualization under image guidance of the masses, allowing the safe passage of the needle and minimising the trauma to the surrounding areas. In biopsy planning, imaging techniques help to define lesion location, accessibility, and suitability for biopsy also providing the identification of the mass to sample, in the context of multiple lesions [6]. In case of metastasis on the liver, not accessible by endoscopy, IR-biopsy can help to identify the primary tumour and define a tissue diagnosis[6].

The choice of imaging guidance modality is multifactorial and there are different options. Ultrasonography (US) is a fast and cost-effective technique, that guarantees real-time imaging, allowing the monitoring of the needle trajectory to the target lesion, without radiation exposure. US-guided percutaneous biopsy provides the diagnosis of solid abdominal organ lesions located in the spleen, pancreas, or lymph nodes, with high diagnostic accuracy and low complications and mortality rates[15]. Moreover, US is useful in guiding biopsies with intracavitary access and must be considered as a diagnostic alternative tool for the diagnosis of low rectal lesions and stromal tumours [16]. The success of US depends on different factors, such as the operator experience [16]. However, different studies suggested US superiority to computed tomography (CT)-guided biopsies, in case of lesions visible with ultrasounds[15,16]. CT-guided biopsy provides a more defined anatomical image, allowing a more precise needle localization when compared to US, showing to be particularly useful in case of pelvic or deep biopsies, which can be difficult to be performed using US. However, CT-guided biopsies have a low real-time guidance capability to track the needle and the target location, requiring intermittent sweeps of the region of interest to confirm the location of the needle during the procedure, thus increasing the biopsy time. The principal disadvantage of the procedure is clearly linked to the radiations exposure expecially for the patients, with radiation dose-related to different factors such as the total scan time, the peak tube kilovoltage (kVP), and milliamperage (mA), the part of the body that must be scanned and the size of the patient[17]. CT-fluoroscopy is an alternative method resulting from technical advantages of the common CT, which allows near real-time imaging of the needled trajectory, reducing the procedural time. Fluoroscopic images are acquired at a lower mA, reducing the radiation dose to the patient, but increasing the radiation dose to the staff, due to the proximity of the physician to the x-ray source during the procedure[18]. However, recent available fusion image guidance systems allow decreasing the radiation exposure through real-time projection during the US-guided biopsies of a needle on to pre-existing CT or magnetic resonance imaging (MRI) image, improving at the same time the accuracy of the procedure[19]. Cone-beam computed tomography (CBCT) guided biopsy, represents the last frontier in the field of IR. Although its extensive use in pleural and pulmonary masses, its virtual navigation system allowed to increase the diagnostic accuracy of the target lesion through a 3D visualization and real-time guidance of the needle trajectory[20], with initial applications also for the diagnosis of GI lesions[21].

IR IN GI CANCERS TREATMENT

Arterial embolization

Arterial embolization (AE) is a useful therapeutic option for hypervascular cancer treatment. Therefore, AE is widely used in liver metastasis treatment, instead of primary GI cancers[22].

Imagine-guided cancer treatment represents a minimally invasive alternative or adjunct to surgery in the management of GI tumours[23,24]. AE consists of the identification of the arterial supply of a solid tumour in CT or MRI and the devascularization of the pathological tissue through transcatheter embolization[24]. Vessels occlusion can be achieved using polyvinyl alcohol, blood clots, coils, and liquid embolic introduced into the tumour bed through fluoroscopic arterial catheterization in IR[25,26]. The interruption of the cancer supplies induced hypoxia and inhibits the tumour growth. Therefore AE can be used in conjunction with ablative treatments or as an alternative to surgery[26]. Indeed, in the case of hypervascular cancers, this technique helps to reduce operative blood loss[27]. AE has a prominent role in the treatment of hepatic metastasis, especially from colon or rectal cancer[28-30]. In this context, a modification of this technique, the TACE, allowed the infusion of a single or combination of chemotherapy agents in the hepatic pathological tissue through the selective hepatic artery embolization[31-33]. This technique reduces the systematic dose of chemotherapy agents, allowing them to reach a higher local concentration. TACE should be repeated for more sessions until the complete devascularization of the pathological tissue[32]. Finally, separate mention should be given to the radioembolization, despite its use is limited to hepatic pathological tissue. It consists of beta-radiation emitting radio-isotopes directly into the mass employing microspheres (glass or resin) resulting in selective tissue necrosis[32].

Ablative techniques

Local cancers ablation is an alternative technique for early stages or not candidate for surgical resection[34]. Tumour ablation mediated by IR allowed pathological tissue necrosis in different modalities, including RF, microwave, and cryotherapy[34]. RF ablation (RFA) is mainly applied in liver metastasis of gastric and colon cancers[35,36]. RFA consists of the administration of electrical energy to a tissue, through an electrode connected in a closed-loop circuit to a monopolar or bipolar energy source [8]. The tissue reached a temperature higher than 60 degrees Celsius with consequent thermal damage. RFA is a safe technique with a lower mortality rate (0.3%) and complication rate (2.2%)[8], with an efficacy, described also in the context of skeletal, renal, and lung metastasis with curative or palliative purpose[37-39]. Conversely to RFA, cryotherapy induces cell necrosis by applying subfreezing temperatures, using nitrogen or argon gas under high pressure[40]. The process of freezing-thawing must be repeated to obtain an effective ablation due to the mechanical stress-induced to the cell membranes[41]. CT identifies the ablated zone in real-time as a low-density area [41]. Acting by a mechanism of osmosis and necrosis, different studies suggested that the intracellular content that remains intact allows inducing an immune-specific reaction with an onco-suppressive effect outside the ablated tissue. However, these considerations are based on preclinical studies[42,43], and prospective clinical trials are needed to confirm these data. Microwave ablation is based on the application of electromagnetic energy within a range of at least 915 MHz, agitating the water molecules in target tissue and inducing cell death through coagulation necrosis[44]. Despite microwave showed equivalent or higher clinical efficacy if compared to RFA, however, RFA showed lower recurrence rates and a higher survival rate achieving extensive necrosis after few sessions, with less post-procedural pain[45,46]. In any case, the decision of which ablation methods should be used, must take into consideration several factors such as the tumour type and location (especially the proximity to vulnerable areas) and patients' comorbidities.

Gene therapy

Advanced in immunology and molecular oncology led to the development of gene therapy. It consists of the administration of genetic agents into a tissue in order to stimulate the immune response, reduce the oncogenic expression, modulate the angiogenesis or modify the response to chemotherapeutics[47]. The selective arterial injections of genetic agents are followed by the vessel embolization, to assure the administration of the substance directly into the mass, limiting the adverse effects and increasing the local dwell time[47]. Genetics agents are typically transferred into the cell through vector agents which allow them to cross cell membranes[48]. Vectors are usually plasmids, phospholipidic agents, or viruses like adenovirus, Epstein-Barr virus, and retroviruses (which provided a lasting genetic expression)[48]. However, clinical studies on gene therapies are very limited and, although the results look promising (especially in the treatment of liver metastases), further studies are needed to confirm the data[48,49].

IR in the treatment of GI cancers complications

IR has also a role in the minimally invasive treatments of different GI cancers complications, avoiding reoperations and allowing a speeding recovery time[50]. Therefore, IR plays a key role in the field of oncology, contributing to revolutionize the postoperative management of these patients. Indeed, IR allows management of possible complications, which would otherwise require a new surgery, in a minimally invasive way.

IR also provides a palliative treatment in advanced GI cancers stages, through diminishing pain or allowing symptoms reduction[9,51].

Bleeding

Besides the role of AE and its modification in the treatment of hepatic pathological tissues, its use in GI cancers is limited to acute bleeding treatments[23,52]. Bleeding from advanced gastric cancers accounts for 1% to 8% of the upper gastrointestinal bleedings (UGIB), causing delays in chemotherapy and increasing transfusion requirements[53,54]. Moreover, endoscopy represents the gold standard for UGIB, being able to recognize the exact source of bleeding[55]. However, in presence of profuse bleeding masking the exact source, endoscopy may fail to stop it[56,57]. Due to advances in angiography systems and haemostatic materials, IR embolization is recognized as an alternative modality in patients in whom endoscopy fails or is not indicated[58,59] IR embolization is also used in the treatment of lower gastrointestinal bleedings (LGIB), defined as bleeding originating distal to the ligament of Treitz[60]. The introduction of super-selective embolization with coaxial microcatheter systems and embolic agents (such as pledgets of absorbable gelatine sponge, polyvinyl alcohol, or other spherical particulates, micro-coils, and liquid embolic agents) represents a useful tool in LGBI[60,61]. According to the American College Guidelines[62] in the treatment of LGIB, it should be considered in high-risk patients with ongoing bleeding who do not respond adequately to the volume resuscitation and who are unlikely to tolerate bowel preparation and colonoscopy (Figure 1). Although its major complication is ischemia, it should be preferred as a first-line approached in these selected patients[63]. A new frontier for the treatment of LGIB is CBCT embolization, which allowed a fast identification of the bleeding site and simplifying the placement of the microcrater in the vessel, without requiring sequential angiography[64]. The indications and possible complications of these techniques are the same as the traditional AE, with the theoretical advantage of greater safety and efficacy due to the modern and accurate tools[64].

AE represents a useful tool also for postoperative bleeding, allowing to stop the bleeding avoiding surgical reoperation, with minimally invasive access[65]. Another possible complication of surgery is the arteriovenous or arterio-enteric fistulas, life-threatening conditions[66]. Although conventional angiography is rarely used as the first-line imaging modality for its diagnosis, angioembolization allowed minimally invasive management of the fistula and to avoid major surgery[67].

Finally, in the event of an arterial bleeding from pseudoanurysm, endovascular treatment with covered self-expanding stent-grafts placement was reported as an effective method. It is performed under local anesthesia, which avoids the need for general or locoregional anesthesia in unstable, high-risk patients[65,66].

Abscess drainage

An intrabdominal abscess could be the first cancer presentation[68] as well as a postoperative complication[50,69]. In both cases, IR is a reliable minimally invasive alternative to surgery, although the feasibility of this technique depends on the abscess location and the consistency of the contents of collections[70]. In case of deep-seated abscess or abscess located close to vulnerable structures, CT-guided percutaneous drainage is the gold standard (Figure 2). Despite the limit of a non-real-time image, it allowed the best image-depiction of the collection and the adjacent organs[7]. In the case of easily accessible abscesses, US-guided drainage must be preferred and should always be the first procedure in patients with simple abscesses[71]. US and CT can be combined with fluoroscopy to avoid guidewire kinking during the procedure and to monitor the placement of catheters[70]. The abscess can only be aspirated, or a catheter can be left in place for few days, especially when contamination or communication with the bowel or urinary tract is suspected[70]. Deep-seated abscess with interposition of organs can be drained with a surgical approach or the intervening organ can be traversed with a catheter[72]. This approach is not suitable for almost all abdominal organs, except the stomach and the liver[72,73]. Finally, transvaginal and transrectal drainage with US or CT guidance allows access to deep-seated abscesses beside the vagina or rectum, often resulting from gynecological or rectal cancers, and inaccessible with percutaneous methods[74,75]. Percutaneous abscess drain placement for abdominal and pelvic collections could be achieved also with cone-beam CT, with equivalent successful rate and radiation dose of conventional CT positioning and the advantage of reduced procedural time[76].

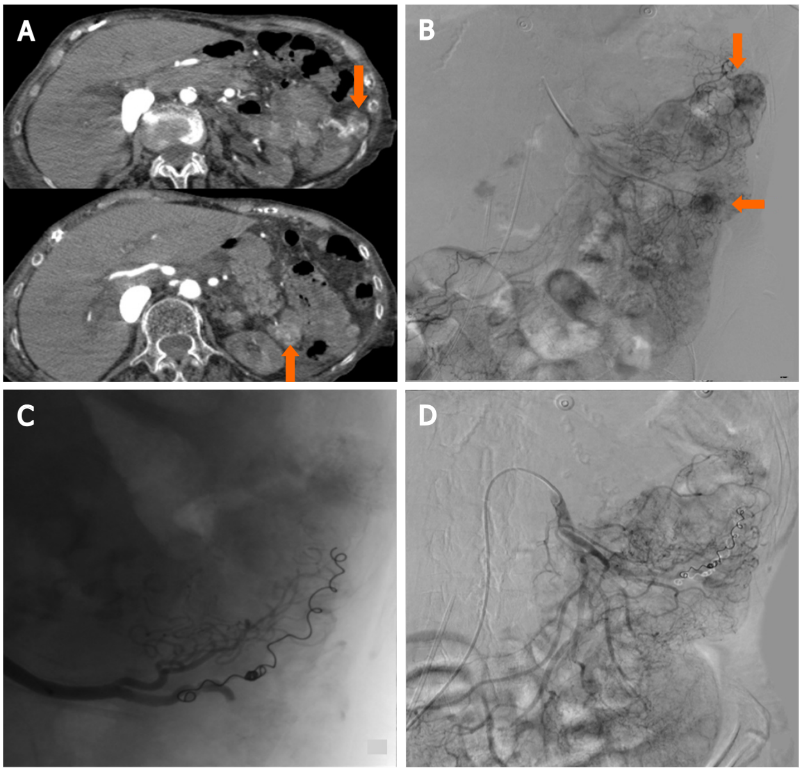

Figure 1 87-year-old female with distal duodenum/proximal jejunum Ca presents with severe recurrent melenas. Endoscopic hemostasis failed in high risk surgical patients with hemodynamic instability and normal coagulation state, requiring embolization after transfusion and hemodynamic stabilization (stabilized blood pressure 90 mmHg with inotropes, HR: 110/min. Hb 6.4). A: Computed tomography-Angio: Two active bleeding sites at proximal jejunum (arrows); B: Selective digital subtraction angiography (DSA) from superior mesenteric artery depicting the bleeding sites (arrows); C: Selective catheterization of the feeding artery with microcatheter and two 3 mm micro coils deployed; D: Lesions are not depicted at final DSA.

GI obstructions

Oesophageal or gastric cancers determining luminal obstruction, dysphagia, or swallowing impairment, are frequently cause of intolerance of the oral intake, requiring nutritional support through a gastrostomy or gastrojejunostomy[77]. The first percutaneous radiologic gastrostomy (PRG) was performed in 1981 using fluoroscopic guidance to avoid bowel and solid organs, without the need for upper endoscopy[10].

IR showed higher technical success and safety rates, with the advantage to be performed in patients not eligible for endoscopy or surgical procedures[10]. PRG complications are similar to the percutaneous endoscopic gastrostomy (PEG), including infections (23%) and the discomfort on feeding (33%)[78,79] and less frequent complications such as haemorrhage, ileus, aspiration of feed, and tube occlusion[10].

The tube dislocation is relatively common, with the possibility of easy tube reinsertion in the same tract if this is established for more than 2 wk. Alternatively, early tube dislodgment requiring repeated gastric puncture[79]. Gastrostomy and gastrojejunostomy can be performed also in small bowel obstruction with a decompression purpose with a success rate higher than 98%[80] (Figure 3). In patients with ascites, a paracentesis must be performed to reduce the peritoneal liquid, to reduce the possibility of complications such as peritonitis or peri-catheter leakage[80,81]. Contraindications for PRG are the same as PEG, including coagulopathy as an absolute contraindication and immunosuppression as a relative one[10]. In the last years, different studies, suggested the positioning of gastroduodenal and colonic self-expanded stent under fluoroscopic-guide as a palliative treatment, in oncologic patients with no indication for surgery[82,83]. Self-expanded stent are extensively used in the palliative treatment of duodenal and rectal occlusions, as given the smallest diameter of these segments, a malignant obstruction can easily occur at these levels [82].

The positioning of the stent under fluoroscopy-guidance allowed to approach the obstruction and the safe placement of the stent, without the need of bowel preparation in case of colonic stents[82]. The use of angiographic catheters with variable head

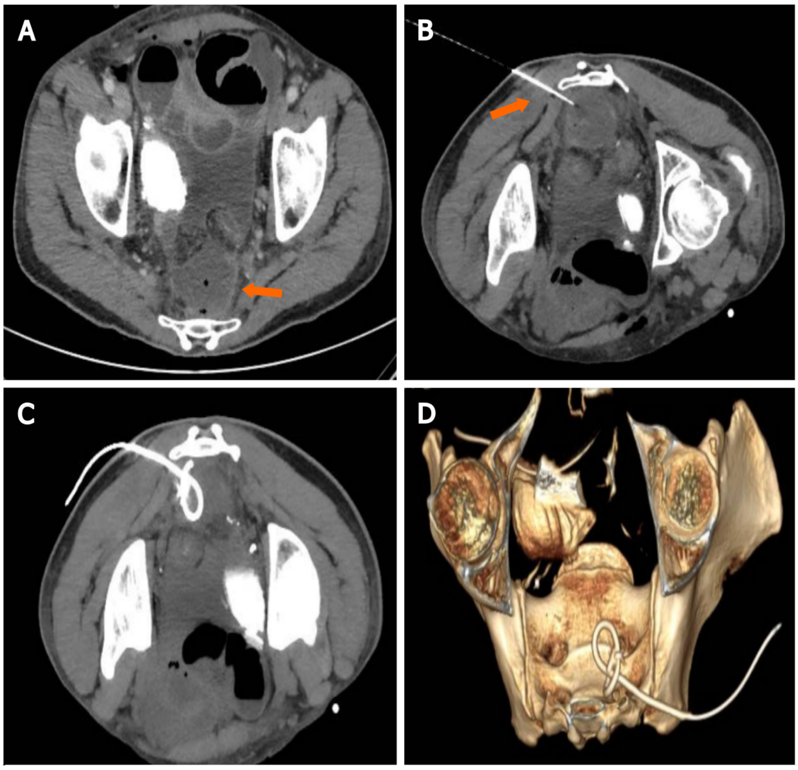

Figure 2 Presacral collection following rectal surgery. A: Axial computed tomography (CT) scan demonstrating a 4 cm × 3 cm presacral fluid collection (arrow), with small air bubbles; B: Patient in prone position, a Chiba needle is inserted with a trans-gluteal approach under CT guidance; C and D: Mip CT images and 3D Volume rendering reconstruction confirming the exact 8Fr drainage positioning.

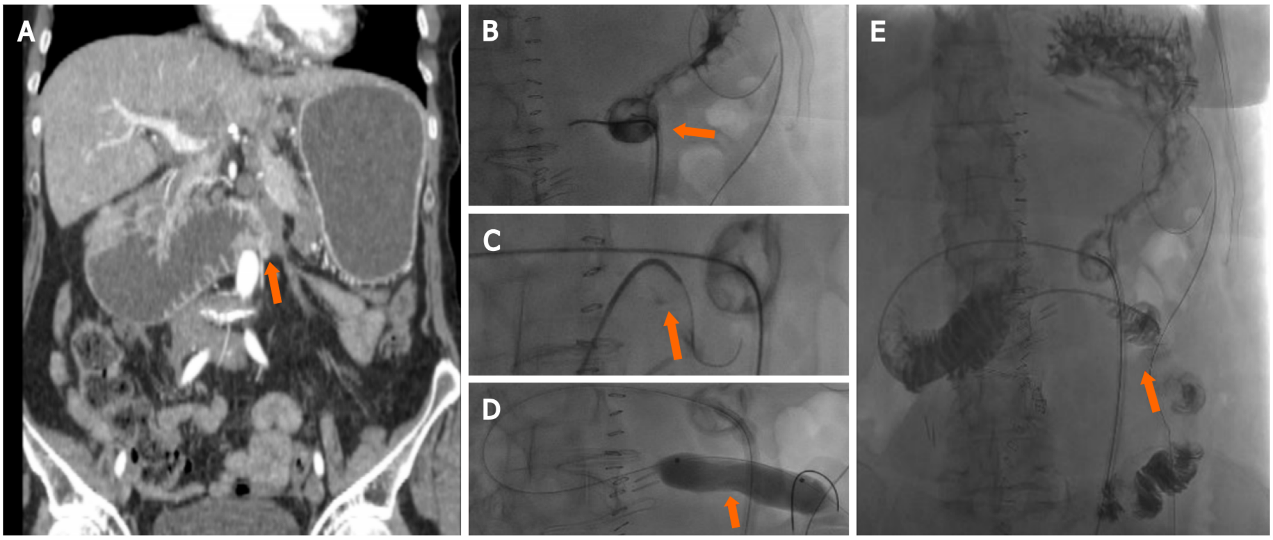

Figure 3 Upper gastrointestinal cancers obstruction. A: A 60 yr female with stage 4 ovarian cancer, with peritoneal carcinomatosis causing occlusion at the Treitz level (arrow); B and C: After percutaneous insertion of a decompressive gastrostomy, an angiografic catheter was advanced at the level of the occlusion and crossed using an hydrophilic guidewire (arrow); D and E: A ballon dilatation (18 mm × 6 cm) was performed (D, arrow) and a 5 fr catheter was left in place to ensure enteral nutrition (E, arrow).

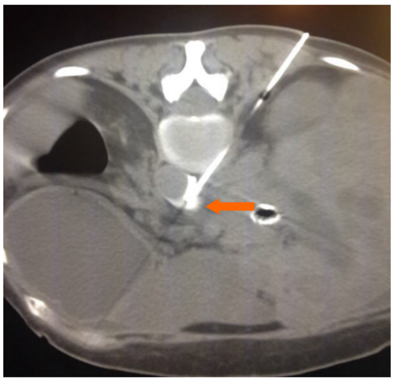

Figure 4 Celiac plexus alcohol neurolysis. In a patient with metastatic pancreatic cancer and non-controlled pain, an 18G Chiba needle (arrow) is inserted under computed tomography-guidance with a paravertebral approach; ethanol (95%–100%) is injected into the antecrural space after confirming the needle position with diluted iodinate contrast medium.

shapes and easily shapable guide-wires can facilitate passing the angulated obstruction, which is the most common cause of endoscopic failure[82,83].

Pain control

Pain represents a significant source of morbidity in oncologic patients, especially in advanced stages, with an incidence ranging from 40% to 90%. According to the World Health Organization, opiates remain the first choice drugs in these patients. However, those patients with non-controlled pain or with intolerable analgesic effects could also benefit from interventional pain control techniques[84,85]. Upper abdominal visceral cancers are often poorly responsive to analgesic therapy. In these cases, nerve block or celiac ganglion neurolysis can reduce pain, especially related to pancreatic, gastric, and oesophageal cancers[86] (Figure 4). The substances most often employed in IR include local alcohol or phenol, which induce permanent nerve destruction, and triamcinolone, which reversibly blocks nocireceptors[87]. CT represents the most commonly used image-modality to guide the celiac axis block, with either an anterior or posterior approach, according to the operator experience[87]. The most frequent complications of these techniques are diarrhea (73%) and orthostatic hypotension (12%)[87].

FUTURE PERSPECTIVES

IR showed an exponential growth in the last years and represents a useful tool in the treatment of oncologic patients. Its role in the context of GI cancers is increasingly relevant, allowing for the diagnosis and treatment of cancer and related complications, with a minimally-invasive approach. The introduction of ablation techniques and monitoring devices contributed to the effectiveness and safety of IR procedures, allowing for the treatment of lesions close to sensitive structures, often difficult to be accessed by other approaches. IR is a very useful tool also in the treatment of GI cancer complications, *e.g.*, bleeding from the digestive tract that cannot be reached by endoscopy[56].

Given the increasing relevance of IR in GI cancers management, the inclusion of interventional radiologists in the multidisciplinary oncologic staff is considered of paramount importance. Specific training programs, also including the use of simulators, are necessary to support the IR learning curve.

CONCLUSION

IR is a medical specialty which uses minimally-invasive technique in GI cancer management. Given its prominent role, the IR specialist should always be considered as an essential player in the multidisciplinary staff responsible for the treatment of the oncologic patient.

ACKNOWLEDGEMENTS

The entire manuscript has been written and amended by a native English speaker (Martin Mariappan MD).

REFERENCES

1 **Arnold M**, Abnet CC, Neale RE, Vignat J, Giovannucci EL, McGlynn KA, Bray F. Global Burden of 5 Major Types of Gastrointestinal Cancer. *Gastroenterology* 2020; **159**: 335-349.e15 [PMID: 32247694 DOI: 10.1053/j.gastro.2020.02.068]

2 **Rawla P**, Barsouk A. Epidemiology of gastric cancer: global trends, risk factors and prevention. *Prz Gastroenterol* 2019; **14**: 26-38 [PMID: 30944675 DOI: 10.5114/pg.2018.80001]

3 **Rawla P**, Sunkara T, Barsouk A. Epidemiology of colorectal cancer: incidence, mortality, survival, and risk factors. *Prz Gastroenterol* 2019; **14**: 89-103 [PMID: 31616522 DOI: 10.5114/pg.2018.81072]

4 **Rawla P**, Sunkara T, Gaduputi V. Epidemiology of Pancreatic Cancer: Global Trends, Etiology and Risk Factors. *World J Oncol* 2019; **10**: 10-27 [PMID: 30834048 DOI: 10.14740/wjon1166]

5 **GBD 2017 Risk Factor Collaborators**. . Global, regional, and national comparative risk assessment of 84 behavioural, environmental and occupational, and metabolic risks or clusters of risks for 195 countries and territories, 1990-2017: a systematic analysis for the Global Burden of Disease Study 2017. *Lancet* 2018; **392**: 1923-1994 [PMID: 30496105 DOI: 10.1016/S0140-6736(18)32225-6]

6 **Silverman SG**, Khorasani R, Adams DF, Phillips MD, Sica GT, Mayer RJ. Multidisciplinary gastrointestinal cancer clinic: abdominal radiologist as active participant. *Acad Radiol* 1998; **5**: 694-697 [PMID: 9787840 DOI: 10.1016/S1076-6332(98)80564-3]

7 **Mahnken AH**, Ricke J. CT- and MR-guided interventions in radiology. Berlin: Springer Berlin Heidelberg, 2013: 11-24

8 **Livraghi T**, Solbiati L, Meloni MF, Gazelle GS, Halpern EF, Goldberg SN. Treatment of focal liver tumors with percutaneous radio-frequency ablation: complications encountered in a multicenter study. *Radiology* 2003; **226**: 441-451 [PMID: 12563138 DOI: 10.1148/radiol.2262012198]

9 **Campbell TC**, Roenn JH. Palliative Care for Interventional Radiology: An Oncologist's Perspective. *Semin Intervent Radiol* 2007; **24**: 375-381 [PMID: 21326589 DOI: 10.1055/s-2007-992325]

10 **Lyon SM**, Pascoe DM. Percutaneous gastrostomy and gastrojejunostomy. *Semin Intervent Radiol* 2004; **21**: 181-189 [PMID: 21331127 DOI: 10.1055/s-2004-860876]

11 **Abi-Jaoudeh N**, Duffy AG, Greten TF, Kohn EC, Clark TW, Wood BJ. Personalized oncology in interventional radiology. *J Vasc Interv Radiol* 2013; **24**: 1083-92; quiz 1093 [PMID: 23885909 DOI: 10.1016/j.jvir.2013.04.019]

12 **Tam AL**, Lim HJ, Wistuba II, Tamrazi A, Kuo MD, Ziv E, Wong S, Shih AJ, Webster RJ 3rd, Fischer GS, Nagrath S, Davis SE, White SB, Ahrar K. Image-Guided Biopsy in the Era of Personalized Cancer Care: Proceedings from the Society of Interventional Radiology Research Consensus Panel. *J Vasc Interv Radiol* 2016; **27**: 8-19 [PMID: 26626860 DOI: 10.1016/j.jvir.2015.10.019]

13 **Mihlon F 4th**, Ray CE Jr, Messersmith W. Chemotherapy agents: a primer for the interventional radiologist. *Semin Intervent Radiol* 2010; **27**: 384-390 [PMID: 22550380 DOI: 10.1055/s-0030-1267852]

14 **de Sio I**, Funaro A, Vitale LM, Niosi M, Francica G, Federico A, Sgambato D, Loguercio C, Romano M. Ultrasound-guided percutaneous biopsy for diagnosis of gastrointestinal lesions. *Dig Liver Dis* 2013; **45**: 816-819 [PMID: 23707404 DOI: 10.1016/j.dld.2013.04.003]

15 **Arellano RS**, Maher M, Gervais DA, Hahn PF, Mueller PR. The difficult biopsy: let's make it easier. *Curr Probl Diagn Radiol* 2003; **32**: 218-226 [PMID: 12963868 DOI: 10.1016/S0363-0188(03)00027-6]

16 **Sheafor DH**, Paulson EK, Simmons CM, DeLong DM, Nelson RC. Abdominal percutaneous interventional procedures: comparison of CT and US guidance. *Radiology* 1998; **207**: 705-710 [PMID: 9609893 DOI: 10.1148/radiology.207.3.9609893]

17 **Cerci JJ**, Tabacchi E, Bogoni M, Delbeke D, Pereira CC, Cerci RJ, Krauzer C, Sakamoto DG, Fanti S, Vitola JV. Comparison of CT and PET/CT for biopsy guidance in oncological patients. *Eur J Nucl Med Mol Imaging* 2017; **44**: 1269-1274 [PMID: 28364161 DOI: 10.1007/s00259-017-3658-8]

18 **Paulson EK**, Sheafor DH, Enterline DS, McAdams HP, Yoshizumi TT. CT fluoroscopy--guided interventional procedures: techniques and radiation dose to radiologists. *Radiology* 2001; **220**: 161-167 [PMID: 11425990 DOI: 10.1148/radiology.220.1.r01jl29161]

19 **Hakime A**, Deschamps F, De Carvalho EG, Teriitehau C, Auperin A, De Baere T. Clinical evaluation of spatial accuracy of a fusion imaging technique combining previously acquired computed tomography and real-time ultrasound for imaging of liver metastases. *Cardiovasc Intervent Radiol* 2011; **34**: 338-344 [PMID: 20845039 DOI: 10.1007/s00270-010-9979-7]

20 **Lim HJ**, Park CM, Yoon SH, Bae JS, Goo JM. Cone-Beam CT Virtual Navigation-Guided Percutaneous Needle Biopsy of Suspicious Pleural Metastasis: A Pilot Study. *Korean J Radiol* 2018; **19**: 872-879 [PMID: 30174476 DOI: 10.3348/kjr.2018.19.5.872]

21 **Choi YR**, Chung JW, Kim JH, Kim HC, Jae HJ, Hur S. Cone-Beam Computed Tomography-Hepatic

Arteriography as a Diagnostic Tool for Small Hypervascular Hepatocellular Carcinomas: Method and Clinical Implications. *Korean J Radiol* 2020; **21**: 306-315 [PMID: 32090523 DOI: 10.3348/kjr.2019.0060]

22 **Takaki H**, Litchman T, Covey A, Cornelis F, Maybody M, Getrajdman GI, Sofocleous CT, Brown KT, Solomon SB, Alago W, Erinjeri JP. Hepatic artery embolization for liver metastasis of gastrointestinal stromal tumor following imatinib and sunitinib therapy. *J Gastrointest Cancer* 2014; **45**: 494-499 [PMID: 25358551 DOI: 10.1007/s12029-014-9663-2]

23 **Goldstein HM**, Medellin H, Ben-Menachem Y, Wallace S. Transcatheter arterial embolization in the management of bleeding in the cancer patient. *Radiology* 1975; **115**: 603-608 [PMID: 1079352 DOI: 10.1148/15.3.603]

24 **Eriksson LG**, Ljungdahl M, Sundbom M, Nyman R. Transcatheter arterial embolization *vs* surgery in the treatment of upper gastrointestinal bleeding after therapeutic endoscopy failure. *J Vasc Interv Radiol* 2008; **19**: 1413-1418 [PMID: 18755604 DOI: 10.1016/j.jvir.2008.06.019]

25 **Amesur NB**, Zajko AB, Carr BI. Chemo-embolization for unresectable hepatocellular carcinoma with different sizes of embolization particles. *Dig Dis Sci* 2008; **53**: 1400-1404 [PMID: 18046645 DOI: 10.1007/s10620-007-9995-x]

26 **Katsanos K**, Kitrou P, Spiliopoulos S, Maroulis I, Petsas T, Karnabatidis D. Comparative effectiveness of different transarterial embolization therapies alone or in combination with local ablative or adjuvant systemic treatments for unresectable hepatocellular carcinoma: A network meta-analysis of randomized controlled trials. *PLoS One* 2017; **12**: e0184597 [PMID: 28934265 DOI: 10.1371/journal.pone.0184597]

27 **Rodríguez Carvajal R**, Orgaz A, Leal JI, Peinado FJ, Vicente S, Gil J, Flores A, Fontcuberta J, Buendia E, Bolufer E, Gómez A, Doblas M. Renal embolization and nephrectomy in a single surgical act in high-risk renal tumor pathology. *Ann Vasc Surg* 2011; **25**: 222-228 [PMID: 20947293 DOI: 10.1016/j.avsg.2010.03.037]

28 **Wörns MA**, Galle PR. Future perspectives in hepatocellular carcinoma. *Dig Liver Dis* 2010; **42** Suppl 3: S302-S309 [PMID: 20547319 DOI: 10.1016/S1590-8658(10)60521-X]

29 **Bruix J**, Gores GJ, Mazzaferro V. Hepatocellular carcinoma: clinical frontiers and perspectives. *Gut* 2014; **63**: 844-855 [PMID: 24531850 DOI: 10.1136/gutjnl-2013-306627]

30 **Fiorentini G**, Sarti D, Nardella M, Inchingolo R, Nestola M, Rebonato A, Guadagni S. Chemoembolization Alone or Associated With Bevacizumab for Therapy of Colorectal Cancer Metastases: Preliminary Results of a Randomized Study. *In Vivo* 2020; **34**: 683-686 [PMID: 32111770 DOI: 10.21873/invivo.11824]

31 **Fiorentini G**, Carandina R, Sarti D, Nardella M, Zoras O, Guadagni S, Inchingolo R, Nestola M, Felicioli A, Barnes Navarro D, Munoz Gomez F, Aliberti C. Polyethylene glycol microspheres loaded with irinotecan for arterially directed embolic therapy of metastatic liver cancer. *World J Gastrointest Oncol* 2017; **9**: 379-384 [PMID: 28979720 DOI: 10.4251/wjgo.v9.i9.379]

32 **Sieghart W**, Hucke F, Peck-Radosavljevic M. Transarterial chemoembolization: modalities, indication, and patient selection. *J Hepatol* 2015; **62**: 1187-1195 [PMID: 25681552 DOI: 10.1016/j.jhep.2015.02.010]

33 **Pereira PL**, Iezzi R, Manfredi R, Carchesio F, Bánsághi Z, Brountzos E, Spiliopoulos S, Echevarria-Uraga JJ, Gonçalves B, Inchingolo R, Nardella M, Pellerin O, Sousa M, Arnold D, de Baère T, Gomez F, Helmberger T, Maleux G, Prenen H, Sangro B, Zeka B, Kaufmann N, Taieb J. The CIREL Cohort: A Prospective Controlled Registry Studying the Real-Life Use of Irinotecan-Loaded Chemoembolisation in Colorectal Cancer Liver Metastases: Interim Analysis. *Cardiovasc Intervent Radiol* 2021; **44**: 50-62 [PMID: 32974773 DOI: 10.1007/s00270-020-02646-8]

34 **Ahmed M**, Solbiati L, Brace CL, Breen DJ, Callstrom MR, Charboneau JW, Chen MH, Choi BI, de Baère T, Dodd GD 3rd, Dupuy DE, Gervais DA, Gianfelice D, Gillams AR, Lee FT Jr, Leen E, Lencioni R, Littrup PJ, Livraghi T, Lu DS, McGahan JP, Meloni MF, Nikolic B, Pereira PL, Liang P, Rhim H, Rose SC, Salem R, Sofocleous CT, Solomon SB, Soulen MC, Tanaka M, Vogl TJ, Wood BJ, Goldberg SN; International Working Group on Image-Guided Tumor Ablation; Interventional Oncology Sans Frontières Expert Panel; Technology Assessment Committee of the Society of Interventional Radiology; Standard of Practice Committee of the Cardiovascular and Interventional Radiological Society of Europe. Image-guided tumor ablation: standardization of terminology and reporting criteria--a 10-year update. *J Vasc Interv Radiol* 2014; **25**: 1691-705.e4 [PMID: 25442132 DOI: 10.1016/j.jvir.2014.08.027]

35 **Chen J**, Tang Z, Dong X, Gao S, Fang H, Wu D, Xiang D, Zhang S. Radiofrequency ablation for liver metastasis from gastric cancer. *Eur J Surg Oncol* 2013; **39**: 701-706 [PMID: 23597495 DOI: 10.1016/j.ejso.2013.03.023]

36 **Liu LX**, Zhang WH, Jiang HC. Current treatment for liver metastases from colorectal cancer. *World J Gastroenterol* 2003; **9**: 193-200 [PMID: 12532430 DOI: 10.3748/wjg.v9.i2.193]

37 **Rose SC**, Thistlethwaite PA, Sewell PE, Vance RB. Lung cancer and radiofrequency ablation. *J Vasc Interv Radiol* 2006; **17**: 927-951; quiz 951 [PMID: 16778226 DOI: 10.1097/01.RVI.0000222707.44902.66]

38 **Thanos L**, Mylona S, Galani P, Tzavoulis D, Kalioras V, Tanteles S, Pomoni M. Radiofrequency ablation of osseous metastases for the palliation of pain. *Skeletal Radiol* 2008; **37**: 189-194 [PMID: 18030464 DOI: 10.1007/s00256-007-0404-5]

39 **Iannuccilli JD**, Dupuy DE, Beland MD, Machan JT, Golijanin DJ, Mayo-Smith WW. Effectiveness and safety of computed tomography-guided radiofrequency ablation of renal cancer: a 14-year single

institution experience in 203 patients. *Eur Radiol* 2016; **26**: 1656-1664 [PMID: 26373755 DOI: 10.1007/s00330-015-4006-7]

40 **Beland M**, Mueller PR, Gervais DA. Thermal ablation in interventional oncology. *Semin Roentgenol* 2007; **42**: 175-190 [PMID: 17599551 DOI: 10.1053/j.ro.2007.04.005]

41 **Aarts BM**, Klompenhouwer EG, Rice SL, Imani F, Baetens T, Bex A, Horenblas S, Kok M, Haanen JBAG, Beets-Tan RGH, Gómez FM. Cryoablation and immunotherapy: an overview of evidence on its synergy. *Insights Imaging* 2019; **10**: 53 [PMID: 31111237 DOI: 10.1186/s13244-019-0727-5]

42 **Chu KF**, Dupuy DE. Thermal ablation of tumours: biological mechanisms and advances in therapy. *Nat Rev Cancer* 2014; **14**: 199-208 [PMID: 24561446 DOI: 10.1038/nrc3672]

43 **Sabel MS**. Cryo-immunology: a review of the literature and proposed mechanisms for stimulatory *vs* suppressive immune responses. *Cryobiology* 2009; **58**: 1-11 [PMID: 19007768 DOI: 10.1016/j.cryobiol.2008.10.126]

44 **Hinshaw JL**, Lubner MG, Ziemlewicz TJ, Lee FT Jr, Brace CL. Percutaneous tumor ablation tools: microwave, radiofrequency, or cryoablation--what should you use and why? *Radiographics* 2014; **34**: 1344-1362 [PMID: 25208284 DOI: 10.1148/rg.345140054]

45 **Galandi D**, Antes G. Radiofrequency thermal ablation *vs* other interventions for hepatocellular carcinoma. *Cochrane Database Syst Rev* 2002; CD003046 [PMID: 12137670 DOI: 10.1002/14651858.CD003046]

46 **Ohmoto K**, Yoshioka N, Tomiyama Y, Shibata N, Kawase T, Yoshida K, Kuboki M, Yamamoto S. Comparison of therapeutic effects between radiofrequency ablation and percutaneous microwave coagulation therapy for small hepatocellular carcinomas. *J Gastroenterol Hepatol* 2009; **24**: 223-227 [PMID: 18823439 DOI: 10.1111/j.1440-1746.2008.05596.x]

47 **Biçeroğlu S**, Memiş A. Gene therapy: applications in interventional radiology. *Diagn Interv Radiol* 2005; **11**: 113-118 [PMID: 15957100]

48 **Yu M**, Chen W, Zhang J. p53 gene therapy for pulmonary metastasis tumor from hepatocellular carcinoma. *Anticancer Drugs* 2010; **21**: 882-884 [PMID: 20679889 DOI: 10.1097/CAD.0b013e32833db1bb]

49 **Mahnken AH**, Pereira PL, de Baère T. Interventional oncologic approaches to liver metastases. *Radiology* 2013; **266**: 407-430 [PMID: 23362094 DOI: 10.1148/radiol.12112544]

50 **Sohn TA**, Yeo CJ, Cameron JL, Geschwind JF, Mitchell SE, Venbrux AC, Lillemoe KD. Pancreaticoduodenectomy: role of interventional radiologists in managing patients and complications. *J Gastrointest Surg* 2003; **7**: 209-219 [PMID: 12600445 DOI: 10.1016/S1091-255X(02)00193-2]

51 **Buss MK**. The Intersection of Palliative Care and Interventional Radiology: Enhancing Understanding and Collaboration. *Semin Intervent Radiol* 2017; **34**: 140-144 [PMID: 28579682 DOI: 10.1055/s-0037-1602756]

52 **Park S**, Shin JH, Gwon DI, Kim HJ, Sung KB, Yoon HK, Ko GY, Ko HK. Transcatheter Arterial Embolization for Gastrointestinal Bleeding Associated with Gastric Carcinoma: Prognostic Factors Predicting Successful Hemostasis and Survival. *J Vasc Interv Radiol* 2017; **28**: 1012-1021 [PMID: 28483303 DOI: 10.1016/j.jvir.2017.03.017]

53 **Del Piano M**, Bianco MA, Cipolletta L, Zambelli A, Chilovi F, Di Matteo G, Pagliarulo M, Ballarè M, Rotondano G; Prometeo study group of the Italian Society of Digestive Endoscopy (SIED). The "Prometeo" study: online collection of clinical data and outcome of Italian patients with acute nonvariceal upper gastrointestinal bleeding. *J Clin Gastroenterol* 2013; **47**: e33-e37 [PMID: 22914349 DOI: 10.1097/MCG.0b013e3182617dcc]

54 **Esrailian E**, Gralnek IM. Nonvariceal upper gastrointestinal bleeding: epidemiology and diagnosis. *Gastroenterol Clin North Am* 2005; **34**: 589-605 [PMID: 16303572 DOI: 10.1016/j.gtc.2005.08.006]

55 **Kim YI**, Choi IJ, Cho SJ, Lee JY, Kim CG, Kim MJ, Ryu KW, Kim YW, Park YI. Outcome of endoscopic therapy for cancer bleeding in patients with unresectable gastric cancer. *J Gastroenterol Hepatol* 2013; **28**: 1489-1495 [PMID: 23662891 DOI: 10.1111/jgh.12262]

56 **Stanley AJ**, Laine L. Management of acute upper gastrointestinal bleeding. *BMJ* 2019; **364**: l536 [PMID: 30910853 DOI: 10.1136/bmj.l536]

57 **Spiliopoulos S**, Inchingolo R, Lucatelli P, Iezzi R, Diamantopoulos A, Posa A, Barry B, Ricci C, Cini M, Konstantos C, Palialexis K, Reppas L, Trikola A, Nardella M, Adam A, Brountzos E. Transcatheter Arterial Embolization for Bleeding Peptic Ulcers: A Multicenter Study. *Cardiovasc Intervent Radiol* 2018; **41**: 1333-1339 [PMID: 29671058 DOI: 10.1007/s00270-018-1966-4]

58 **Lee HJ**, Shin JH, Yoon HK, Ko GY, Gwon DI, Song HY, Sung KB. Transcatheter arterial embolization in gastric cancer patients with acute bleeding. *Eur Radiol* 2009; **19**: 960-965 [PMID: 18987861 DOI: 10.1007/s00330-008-1216-2]

59 **Inchingolo R**, Nestola M, Posa A, Di Costanzo G, Nardella M. Intrastent Pseudoaneurysm following Endoscopic Biliary Stent Insertion. *J Vasc Interv Radiol* 2017; **28**: 1321-1323 [PMID: 28841953 DOI: 10.1016/j.jvir.2017.04.014]

60 **Speir EJ**, Ermentrout RM, Martin JG. Management of Acute Lower Gastrointestinal Bleeding. *Tech Vasc Interv Radiol* 2017; **20**: 258-262 [PMID: 29224658 DOI: 10.1053/j.tvir.2017.10.005]

61 **Hur S**, Jae HJ, Lee M, Kim HC, Chung JW. Safety and efficacy of transcatheter arterial embolization for lower gastrointestinal bleeding: a single-center experience with 112 patients. *J Vasc Interv Radiol* 2014; **25**: 10-19 [PMID: 24286939 DOI: 10.1016/j.jvir.2013.09.012]

62 **Strate LL**, Gralnek IM. ACG Clinical Guideline: Management of Patients With Acute Lower Gastrointestinal Bleeding. *Am J Gastroenterol* 2016; **111**: 459-474 [PMID: 26925883 DOI: 10.1038/ajg.2016.41]

63 **Nykänen T**, Peltola E, Kylänpää L, Udd M. Transcatheter Arterial Embolization in Lower Gastrointestinal Bleeding: Ischemia Remains a Concern Even with a Superselective Approach. *J Gastrointest Surg* 2018; **22**: 1394-1403 [PMID: 29549618 DOI: 10.1007/s11605-018-3728-7]

64 **Ierardi AM**, Urbano J, De Marchi G, Micieli C, Duka E, Iacobellis F, Fontana F, Carrafiello G. New advances in lower gastrointestinal bleeding management with embolotherapy. *Br J Radiol* 2016; **89**: 20150934 [PMID: 26764281 DOI: 10.1259/bjr.20150934]

65 **Chatani S**, Inoue A, Ohta S, Takaki K, Sato S, Iwai T, Murakami Y, Watanabe S, Sonoda A, Nitta N, Maehira H, Tani M, Murata K. Transcatheter Arterial Embolization for Postoperative Bleeding Following Abdominal Surgery. *Cardiovasc Intervent Radiol* 2018; **41**: 1346-1355 [PMID: 29955913 DOI: 10.1007/s00270-018-2019-8]

66 **Partovi S**, Trischman T, Sheth RA, Huynh TTT, Davidson JC, Prabhakar AM, Ganguli S. Imaging work-up and endovascular treatment options for aorto-enteric fistula. *Cardiovasc Diagn Ther* 2018; **8**: S200-S207 [PMID: 29850432 DOI: 10.21037/cdt.2017.10.05]

67 **Chiesa R**, Melissano G, Marone EM, Marrocco-Trischitta MM, Kahlberg A. Aorto-oesophageal and aortobronchial fistulae following thoracic endovascular aortic repair: a national survey. *Eur J Vasc Endovasc Surg* 2010; **39**: 273-279 [PMID: 20096612 DOI: 10.1016/j.ejvs.2009.12.007]

68 **Cho J**, Park I, Lee D, Sung K, Baek J, Lee J. Advanced Gastric Cancer Perforation Mimicking Abdominal Wall Abscess. *J Gastric Cancer* 2015; **15**: 214-217 [PMID: 26468420 DOI: 10.5230/jgc.2015.15.3.214]

69 **Connell TR**, Stephens DH, Carlson HC, Brown ML. Upper abdominal abscess: a continuing and deadly problem. *AJR Am J Roentgenol* 1980; **134**: 759-765 [PMID: 6767363 DOI: 10.2214/ajr.134.4.759]

70 **Maher MM**, Gervais DA, Kalra MK, Lucey B, Sahani DV, Arellano R, Hahn PF, Mueller PR. The inaccessible or undrainable abscess: how to drain it. *Radiographics* 2004; **24**: 717-735 [PMID: 15143224 DOI: 10.1148/rg.243035100]

71 **Men S**, Akhan O, Köroğlu M. Percutaneous drainage of abdominal abcess. *Eur J Radiol* 2002; **43**: 204-218 [PMID: 12204403 DOI: 10.1016/S0720-048X(02)00156-0]

72 **Cronin CG**, Gervais DA, Castillo CF, Mueller PR, Arellano RS. Interventional radiology in the management of abdominal collections after distal pancreatectomy: a retrospective review. *AJR Am J Roentgenol* 2011; **197**: 241-246 [PMID: 21701036 DOI: 10.2214/AJR.10.5447]

73 **Hawel J**, McFadgen H, Stewart R, El-Ghazaly T, Alawashez A, Ellsmere J. Interventional radiology-assisted transgastric endoscopic drainage of peripancreatic fluid collections. *Can J Surg* 2020; **63**: E254-E256 [PMID: 32400149 DOI: 10.1503/cjs.003019]

74 **Varghese JC**, O'Neill MJ, Gervais DA, Boland GW, Mueller PR. Transvaginal catheter drainage of tuboovarian abscess using the trocar method: technique and literature review. *AJR Am J Roentgenol* 2001; **177**: 139-144 [PMID: 11418415 DOI: 10.2214/ajr.177.1.1770139]

75 **Martins BC**, Marques CF, Nahas CS, Hondo FY, Pollara W, Nahas SC, Ribeiro Junior U, Cecconello I, Maluf-Filho F. A novel approach for the treatment of pelvic abscess: transrectal endoscopic drainage facilitated by transanal endoscopic microsurgery access. *Surg Endosc* 2012; **26**: 2667-2670 [PMID: 22407154 DOI: 10.1007/s00464-012-2215-6]

76 **Partovi S**, Li X, Moon E, Thompson D. Image guided percutaneous gastrostomy catheter placement: How we do it safely and efficiently. *World J Gastroenterol* 2020; **26**: 383-392 [PMID: 32063687 DOI: 10.3748/wjg.v26.i4.383]

77 **McKay T**, Ingraham CR, Johnson GE, Kogut MJ, Vaidya S, Padia SA. Cone-Beam CT with Fluoroscopic Overlay Versus Conventional CT Guidance for Percutaneous Abdominopelvic Abscess Drain Placement. *J Vasc Interv Radiol* 2016; **27**: 52-57 [PMID: 26573489 DOI: 10.1016/j.jvir.2015.09.016]

78 **Gonçalves F**, Mozes M, Saraiva I, Ramos C. Gastrostomies in palliative care. *Support Care Cancer* 2006; **14**: 1147-1151 [PMID: 16625334 DOI: 10.1007/s00520-006-0045-6]

79 **Silas AM**, Pearce LF, Lestina LS, Grove MR, Tosteson A, Manganiello WD, Bettmann MA, Gordon SR. Percutaneous radiologic gastrostomy *vs* percutaneous endoscopic gastrostomy: a comparison of indications, complications and outcomes in 370 patients. *Eur J Radiol* 2005; **56**: 84-90 [PMID: 16168268 DOI: 10.1016/j.ejrad.2005.02.007]

80 **Ryan JM**, Hahn PF, Mueller PR. Performing radiologic gastrostomy or gastrojejunostomy in patients with malignant ascites. *AJR Am J Roentgenol* 1998; **171**: 1003-1006 [PMID: 9762985 DOI: 10.2214/ajr.171.4.9762985]

81 **Given MF**, Lyon SM, Lee MJ. The role of the interventional radiologist in enteral alimentation. *Eur Radiol* 2004; **14**: 38-47 [PMID: 12736755 DOI: 10.1007/s00330-003-1911-y]

82 **Katsanos K**, Sabharwal T, Adam A. Stenting of the lower gastrointestinal tract: current status. *Cardiovasc Intervent Radiol* 2011; **34**: 462-473 [PMID: 21127865 DOI: 10.1007/s00270-010-0005-x]

83 **Katsanos K**, Sabharwal T, Adam A. Stenting of the upper gastrointestinal tract: current status. *Cardiovasc Intervent Radiol* 2010; **33**: 690-705 [PMID: 20521050 DOI: 10.1007/s00270-010-9862-6]

84 **Caraceni A**, Portenoy RK; a working group of the IASP Task Force on Cancer Pain. An international survey of cancer pain characteristics and syndromes. IASP Task Force on Cancer Pain. International Association for the Study of Pain. *Pain* 1999; **82**: 263-274 [PMID: 10488677 DOI: 10.1016/S0304-3959(99)00073-1]

85 **Caraceni A**, Martini C, Zecca E, Portenoy RK, Ashby MA, Hawson G, Jackson KA, Lickiss N, Muirden N, Pisasale M, Moulin D, Schulz VN, Rico Pazo MA, Serrano JA, Andersen H, Henriksen HT, Mejholm I, Sjogren P, Heiskanen T, Kalso E, Pere P, Poyhia R, Vuorinen E, Tigerstedt I,

Ruismaki P, Bertolino M, Larue F, Ranchere JY, Hege-Scheuing G, Bowdler I, Helbing F, Kostner E, Radbruch L, Kastrinaki K, Shah S, Vijayaram S, Sharma KS, Devi PS, Jain PN, Ramamani PV, Beny A, Brunelli C, Maltoni M, Mercadante S, Plancarte R, Schug S, Engstrand P, Ovalle AF, Wang X, Alves MF, Abrunhosa MR, Sun WZ, Zhang L, Gazizov A, Vaisman M, Rudoy S, Gomez Sancho M, Vila P, Trelis J, Chaudakshetrin P, Koh ML, Van Dongen RT, Vielvoye-Kerkmeer A, Boswell MV, Elliott T, Hargus E, Lutz L; Working Group of an IASP Task Force on Cancer Pain. Breakthrough pain characteristics and syndromes in patients with cancer pain. An international survey. *Palliat Med* 2004; **18**: 177-183 [PMID: 15198130 DOI: 10.1191/0269216304pm890oa]

86 **Midia M**, Dao D. The Utility of Peripheral Nerve Blocks in Interventional Radiology. *AJR Am J Roentgenol* 2016; **207**: 718-730 [PMID: 27385059 DOI: 10.2214/AJR.16.16643]

87 **Akhan O**, Ozmen MN, Basgun N, Akinci D, Oguz O, Koroglu M, Karcaaltincaba M. Long-term results of celiac Ganglia block: correlation of grade of tumoral invasion and pain relief. *AJR Am J Roentgenol* 2004; **182**: 891-896 [PMID: 15039160 DOI: 10.2214/ajr.182.4.1820891]

World Journal of Radiology

Submit a Manuscript: https://www.f6publishing.com

World J Radiol 2021 October 28; 13(10): 327-343

DOI: 10.4329/wjr.v13.i10.327

ISSN 1949-8470 (online)

MINIREVIEWS

COVID-19 pneumonia: A review of typical radiological characteristics

María Churruca, Elisa Martínez-Besteiro, Felipe Couñago, Pedro Landete

ORCID number: María Churruca 0000-0001-6198-3619; Elisa Martínez-Besteiro 0000-0002-2968-1271; Felipe Couñago 0000-0001-7233-0234; Pedro Landete 0000-0002-9631-9408.

Author contributions: All authors contributed to this paper with conception and design of the manuscript, literature review and analysis, drafting and critical revision and editing, and final approval of the final version.

Conflict-of-interest statement: Authors declare no potential conflict of interests for this article.

Manuscript source: Invited manuscript

Specialty type: Radiology, nuclear medicine and medical imaging

María Churruca, Elisa Martínez-Besteiro, Pulmonology Department, Hospital Universitario de La Princesa, Madrid 28006, Spain

Felipe Couñago, Department of Radiation Oncology, Hospital Universitario Quirónsalud Madrid, Madrid 28223, Spain

Felipe Couñago, Department of Radiation Oncology, Hospital La Luz, Madrid 28003, Spain

Felipe Couñago, Clinical Department, Faculty of Biomedicine,Universidad Europea de Madrid, Madrid 28670, Spain

Pedro Landete, Department of Pneumology, Hospital Universitario de la Princesa, Universidad Autónoma de Madrid, Madrid 28006, Spain

Corresponding author: María Churruca, MD, Doctor, Pulmonology Department, Hospital Universitario de La Princesa, Diego de León 62, Madrid 28006, Spain. mchurrucaarrospide@gmail.com

Abstract

Coronavirus disease 2019 (COVID-19) was first discovered after unusual cases of severe pneumonia emerged by the end of 2019 in Wuhan (China) and was declared a global public health emergency by the World Health Organization in January 2020. The new pathogen responsible for the infection, genetically similar to the beta-coronavirus family, is known as severe acute respiratory syndrome coronavirus-2 (SARS-CoV-2), and the current gold standard diagnostic tool for its detection in respiratory samples is the reverse transcription-polymerase chain reaction test. Imaging findings on COVID-19 have been widely described in studies published throughout last year, 2020. In general, ground-glass opacities and consolidations, with a bilateral and peripheral distribution, are the most typical patterns found in COVID-19 pneumonia. Even though much of the literature focuses on chest computed tomography (CT) and X-ray imaging and their findings, other imaging modalities have also been useful in the assessment of COVID-19 patients. Lung ultrasonography is an emerging technique with a high sensitivity, and thus useful in the initial evaluation of SARS-CoV-2 infection. In addition, combined positron emission tomography-CT enables the identification of affected areas and follow-up treatment responses. This review intends to clarify the role of the imaging modalities available and identify the most common radiological manifestations of COVID-19.

Key Words: COVID-19; Radiology; Chest X-ray; Lung ultrasonography; Computed

Country/Territory of origin: Spain

Peer-review report's scientific quality classification

Grade A (Excellent): 0
Grade B (Very good): B
Grade C (Good): C
Grade D (Fair): 0
Grade E (Poor): 0

Received: January 25, 2021
Peer-review started: January 25, 2021
First decision: March 1, 2021
Revised: March 8, 2021
Accepted: September 14, 2021
Article in press: September 14, 2021
Published online: October 28, 2021

P-Reviewer: Bhardwaj R, Grassi R
S-Editor: Gong ZM
L-Editor: A
P-Editor: Liu JH

Tomography; Positron emission tomography-computed tomography

Core Tip: Severe acute respiratory syndrome coronavirus-2 is a single-stranded RNA virus that was first isolated in December 2019. Currently, the reverse transcription-polymerase chain reaction test, performed on respiratory samples collected in suspected coronavirus disease 2019 (COVID-19) patients, is the gold standard diagnostic technique. Chest X-ray or computed tomography (CT) are the main imaging tests used to diagnose COVID-19 pneumonia, with ground-glass opacities and consolidations being the major imaging features encountered. There are other radiological modalities, such as lung ultrasonography and combined positron emission tomography-CT, that can provide further information for initial assessment and follow-up treatment response.

Citation: Churruca M, Martínez-Besteiro E, Couñago F, Landete P. COVID-19 pneumonia: A review of typical radiological characteristics. *World J Radiol* 2021; 13(10): 327-343
URL: https://www.wjgnet.com/1949-8470/full/v13/i10/327.htm
DOI: https://dx.doi.org/10.4329/wjr.v13.i10.327

INTRODUCTION

On 31 December 2019, 27 cases of pneumonia of unknown aetiology were identified in the city of Wuhan (Hubei Province, China). A new pathogen, genetically similar to the beta-coronavirus family to which the coronaviruses that caused previous epidemics belong – severe acute respiratory syndrome coronavirus (SARS-CoV) and Middle East respiratory syndrome (MERS-CoV) – was isolated from collected respiratory samples and named severe acute respiratory syndrome coronavirus-2 (SARS-CoV-2). In January 2020, the World Health Organization named the disease Coronavirus disease 2019 (COVID-19) and declared a global public health emergency[1,2]. At the beginning of December 2020, a total of 65.8 million cases had been diagnosed, with 1.5 million confirmed deaths since the start of the pandemic[3].

The clinical presentation and radiological findings of COVID-19, as well as various diagnostic tools for its detection, have been widely described in multiple studies published throughout 2020. Regarding its clinical pattern, it is generally nonspecific and variable between individuals. In approximately 80%-90% of cases, the disease is mild or even asymptomatic. However, in the remaining approximately 10% of cases, generally frail patients with coexisting medical conditions develop a severe course of infection with dyspnoea, hypoxaemia and extensive radiological lung involvement[4] . The current gold standard diagnostic tool for the detection of SARS-CoV-2 RNA in respiratory samples is the reverse transcription-polymerase chain reaction (RT-PCR) test. This test shows a non-negligible rate of false negatives results, which can be attributed to errors in the extraction of nasopharyngeal swab sampling and when the sample is collected[5], since its sensitivity varies depending on the time since exposure. Thus, some studies estimate the sensitivity of the RT-PCR test to be 33% four days after exposure, 62% the day clinical manifestations begin and 80% three days after the onset of symptoms[6]. A combination of the growing and rapid spread of COVID-19 and the lack of RT-PCR testing kits in some affected areas has made new diagnostic and screening methods necessary[7]. Radiological diagnosis constitutes an essential component in the initial assessment of the extension and severity of the infection, as it is a key element to guide treatment and monitor the evolution of the condition[8]. So far, much of the literature has predominantly focused on characterising the radiological findings most frequently seen in chest computed tomography (CT). However, other diagnostic modalities, such as chest X-ray, lung ultrasonography (LUS) and combined positron emission tomography-computed tomography (PET-CT), have also been useful in the assessment and management of COVID-19 patients[5].

Ultimately, clinicians will choose an imaging modality based on its advantages, the experience gathered with each diagnostic method and the local resources available[9]. This review aims to clarify the diagnostic value of the different imaging modalities available and describe the most common radiological findings in COVID-19.

CHEST X-RAY

Chest X-ray is a frequently used method due to its low cost and wide availability, allowing various conditions to be studied in a simple and fast manner.

Furthermore, the existence of portable X-ray devices has enabled its use in intensive care units (ICUs). It is important that clinicians understand both the advantages and limitations of this imaging technique in terms of diagnosing COVID-19 pneumonia [10].

Some studies have proposed that chest radiography is a useful method both for the diagnosis and follow-up of the lung pathology generated by SARS-CoV-2 infection. The American College of Radiology (ACR) defends the application of portable X-rays in order to avoid collapses in imaging departments and minimise the risk of contamination associated with the intra-hospital mobilisation of COVID-19 patients and thus the spread of the disease[11].

Studies published during 2020 report a low sensitivity of chest X-rays in detecting pulmonary infiltrates during the initial phases of COVID-19 infection, as well as in mild forms of the disease (Table 1)[12]. In this regard, in a retrospective study of 64 patients, Wong *et al*[13] noted a chest radiography sensitivity of just 69%, compared to 91% for the RT-PCR test, and highlighted that 9% of cases in which X-ray detected abnormalities were initially RT-PCR negative. Both Ng *et al*[14] and Kim *et al*[15] found that chest X-ray has a low sensitivity when it comes to identifying lung alterations caused by SARS-CoV-2 infection. However, at the beginning of February, Chen *et al*[16] published a study which found a sensitivity of 100% with the use of chest radiography, with 74/99 patients presenting bilateral pneumonia and 25/99 unilateral involvement. However, these results can be explained by the overload that the health system was experiencing at that time, when the radiological screening of positive COVID-19 patients was limited to severe and advanced cases. For these reasons, the European Society of Radiology and the European Society of Thoracic Imaging recommend avoiding its use as a first-line technique in the diagnosis of COVID-19 pneumonia, restricting its use to the follow-up of patients admitted to the ICU, whose fragility would make it difficult to transfer them for a chest CT scan[11].

The severity of COVID-19 pneumonia cannot be determined by a SARS-CoV-2-positive nasopharyngeal swab; therefore, it is necessary to conduct a complementary radiological study. Recently, Cellina *et al*[17] retrospectively studied the prognostic predictive value of radiographic imaging performed in the initial stages of the disease in 246 COVID-19 patients, establishing a significant correlation between lung parenchymal involvement – valued by a percentage of the areas affected by ground-glass opacities (GGOs) or consolidation – and the severity of the disease.

The most common manifestations found in the chest radiographs of COVID-19 patients are GGOs – sometimes accompanied by reticular opacities – and lung consolidation, which, as in other atypical viral pneumonias, are typically multilobar and bilateral, generally involving the lower lobes (Table 2). One of the most specific signs of COVID-19 pneumonia is the peripheral and multifocal location of pulmonary infiltrates (Figure 1). Radiological impairments can rapidly evolve into a consolidative pattern, frequently reaching the peak of maximum severity and the worst pulmonary parenchymal involvement between 6-12 d after the onset of symptoms (Figure 2). Pleural effusion is extremely rare in patients infected by SARS-CoV-2, but if detected, is normally identified in the late stages of the disease. Lung cavitation images and pneumothorax are also unusual but can occur in some COVID-19 cases (Figure 3)[18]. Lomoro *et al*[19] retrospectively studied the chest X-rays of 32 patients, describing consolidations in 46.9% of the cases and GGOs in 37.5%, without identifying pleural effusion in any of them. The distribution of these findings was predominately bilateral (78.1%) and unilateral only in 6.2% of the cases. Furthermore, the lower lobes were the most frequently affected (52%), followed by 34.4% of patients who presented similar involvement of both the upper and lower lobes, while just 3.1% presented involvement in the upper lobes.

The impact of pneumomediastinum and subcutaneous emphysema during the COVID-19 pandemic has been described by Lemmers *et al*[20], who detected these conditions in 13% of the patients in their study. While at the outset this was considered to be a consequence of the barotrauma produced by mechanical ventilation in critically ill respiratory patients, it is nevertheless believed that these findings could be attributed to the Macklin effect, characterised by the rupture of the pulmonary alveoli

Table 1 Adapted from Chen *et al*[21] chest X-ray sensitivity in coronavirus disease 2019 pneumonia

Ref.	Cases	Initial RT-PCR	RT-PCR	Abnormal	Bilateral
Wong *et al*[13], 2020	64	Positive 58/64 (91%); Negative 6/64 (9%)	64 positive/0 negative	21/64 (33%)	32/64 (50%)
Chen *et al*[21], 2020	99	–	99 positive/0 negative	99/99 (100%)	74/99 (75%)
Kim *et al*[15], 2020	28	–	28 positive/ 0 negative	13/28 (46.4%)	6 (21.4%)
Ng *et al*[14], 2020	21	–	21 positive/0 negative	3/5 (60%)	2/5 (40%)

RT-PCR: Reverse transcription-polymerase chain reaction.

Table 2 Most common findings of chest X-rays

Main distribution	
Bilateral	+++
Unilateral	+
Imaging findings	
Ground-glass opacities	++++
Consolidation	+++
Reticular opacities	+++
Pneumothorax/pneumomediastinum	++
Pleural effusion	+
Lung cavitation	+

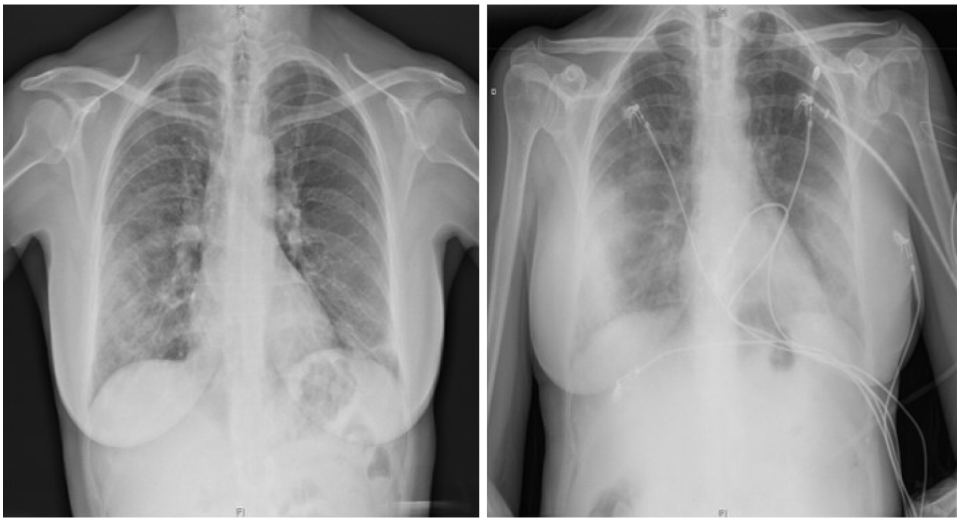

Figure 1 Chest X-ray findings in a 60-year-old woman with confirmed severe acute respiratory syndrome coronavirus-2 pneumonia (positive RT-PCR test). PA X-ray (left) with patchy right mid-to-lower and left lower lung opacities. AP X-ray (right) with peripherally distributed bilateral lung opacities.

– fragile in these patients – which releases air that centripetally dissects through the pulmonary interstitium, reaching the mediastinum.

Ultimately, the published data suggest that chest radiography has a high utility in patients with SARS-CoV-2 infection, especially in those with moderate to severe pulmonary involvement and in the advanced stages of the disease. Moreover, it can serve as a first-line imaging tool when resources are limited, playing a key role in the monitoring of patients and the evaluation of eventual associated complications[21].

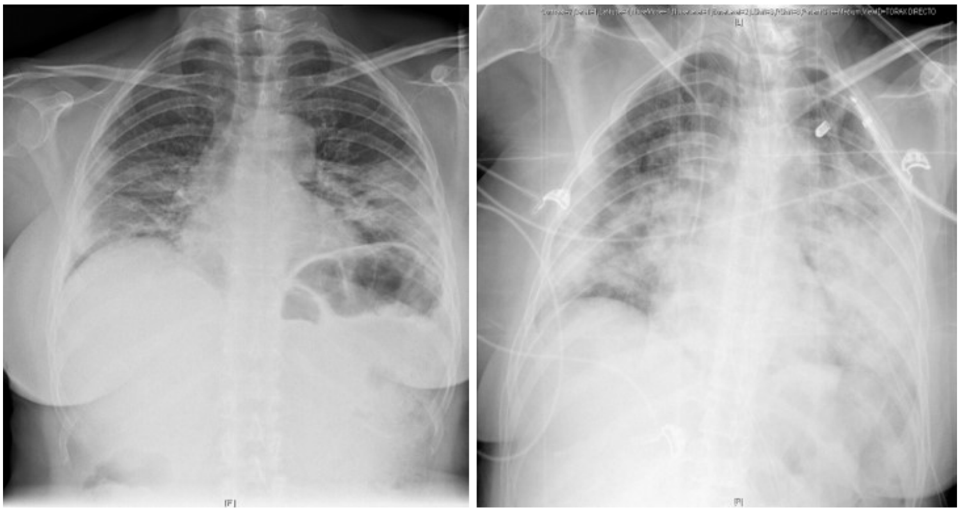

Figure 2 PA Chest X-ray findings in a 55-year-old woman with varying degrees of coronavirus disease 2019 pneumonia defined by diffuse ground-glass and consolidative opacities, predominantly involving the lower zone in both lungs.

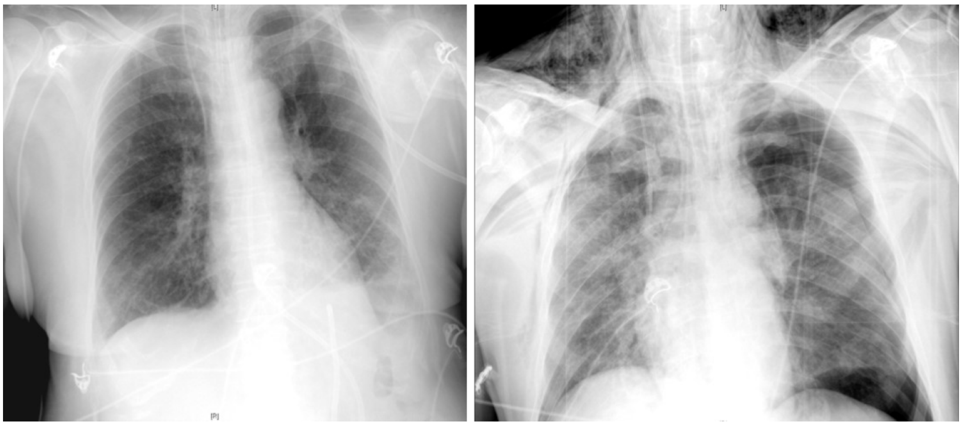

Figure 3 AP chest X-ray findings. AP chest X-ray findings (left) in an 80-year-old man with bilateral COVID-19 pneumonia and associated left pleural effusion. AP chest X-ray findings (right) in an 84-year-old man with bilateral alveolar infiltrates, diffusely distributed and left tension pneumothorax with subcutaneous emphysema.

LUNG ULTRASONOGRAPHY IN THE COVID-19 ERA

Since the influenza A pandemic (H1N1) in 2009 and the avian influenza epidemic (H7N9) in 2013, LUS has become a significant diagnostic tool for the early detection of interstitial lung disease[22,23]. The current data published on COVID-19 support it as a safe and accessible emerging technique that can be applied to patients with either suspected or confirmed SARS-CoV-2 infection, both in the initial evaluation and the subsequent follow-up.

Traditionally, a healthy lung is considered invisible to ultrasonography. Since it is an aerated organ, it does not transmit ultrasound and therefore does not provide anatomical images. However, when lung tissue is occupied by fluid or cellular elements, its impedance varies resulting in artifacts that permit the identification of pathological findings.

The most basic of these artifacts are *A lines* – transversal hyperechoic lines parallel to the pleural line – separated by a distance equal to that between the pleural line and the skin. They are the result of the reverberation of the pleural line in a healthy lung, representing normal lung aeration.

An additional and significant artifact in LUS are *B lines*, which are described as vertical hyperechogenic artifacts that arise from the pleural line. They extend like a comet tail towards the deep parenchyma, hiding *A lines* on their way and moving synchronously with pleural sliding[24]. They are considered to be the main ultrasound sign of interstitial lung disease, and their quantity increases as air content decreases and lung density intensifies. The presence of more than three *B lines* per intercostal space is considered pathological.

In normal conditions, the pleural line is hyperechogenic, thin and regular. However, in the presence of inflammation, thickening and/or fragmentation may occur if there are adjacent pulmonary consolidations. Additionally, there may be a decrease in pleural sliding.

One of the great advantages of LUS is its accessibility and immediacy, since it generates bedside and real-time images. Additionally, it is a non-invasive and innocuous technique that can be applied safely in certain population groups, such as pregnant women and paediatric patients.

Furthermore, LUS has a high sensitivity and outperforms chest X-rays in detecting the early stages of interstitial lung disease[25].

The main limitation of LUS is its operator-dependent nature, as its reliability is closely related to clinicians' experience and ability. However, in experienced hands, the whole exploration can be performed in a few minutes, thus providing results faster in comparison with other imaging tests.

Lung ultrasound patterns in COVID-19

Before the outbreak of the COVID-19 pandemic, previous studies reported that LUS findings were highly consistent with chest CTs in patients with viral pneumonia[26]. Similarly, in patients with SARS-CoV-2 pneumonia, there is a good correlation between both imaging techniques[27-31].

The common ultrasound findings described in patients with SARS-CoV-2 infection are summarised in Table 3 and Figure 4[32,33].

Gattinoni *et al*[34] describe two different ultrasound patterns in the hyperinflammatory phase of COVID-19: One phenotype of diffuse pulmonary infiltrates (type L), with normal or minimally decreased lung compliance, and therefore limited scope for alveolar recruitment, and a second phenotype of extensive consolidations (type H), with a low or very low compliance and with a clinical and prognostic behaviour analogous to the common acute respiratory distress syndrome (ARDS).

None of the findings described so far are pathognomonic for COVID-19; therefore, LUS cannot provide a confirmatory diagnosis. As such, it is essential to integrate the images with a clinical assessment and nasopharyngeal swab result.

Recently, some authors have discovered an unusual finding that could be more specific to COVID-19: The '*light beam*'[35]. This is a thick hyperechogenic band of confluent *B lines* that originates from a portion of the pleural line that is apparently preserved. It is usually found in the early stages of the disease and correlates with incipient GGOs on chest CT scan.

LUS findings vary depending on the stage of the disease (Figure 5)[36]. Thus, in the first days after the onset of symptoms, it is common to observe unilateral or bilateral focal *B lines.* As the disorder progresses, the density of lung parenchyma increases along with the number of *B lines*; diffuse and bilateral *B lines* appear, starting from a pleural line that begins to thicken and becomes irregular, with small subpleural consolidations. Finally, *B lines* may coalesce, creating a 'white lung' pattern of consolidation or hepatisation of the lung parenchyma – particularly in declining areas – with the respiratory failure that this implies.

Given its high sensitivity, LUS allows the detection of both deterioration and recovery in lung lesions during the final stage of the disease. Consequently, during the convalescent stage, there is a progressive regression of *B lines* and consolidations. Additionally, *A lines* appear one again, in accordance with aeration improvement[31].

LUS is also efficient for the assessment of other events that, although not common, can occur in the course of SARS-CoV-2 pneumonia. These events include pleural effusion, pneumothorax – associated with mechanical ventilation or the insertion of a central venous catheter, among other causes – or a pulmonary embolism (PE). CT pulmonary angiogram remains the gold standard technique for the diagnosis of PE, but in critical, unstable patients with a suspected diagnosis, ultrasounds can provide valuable information on the presence of right ventricular dysfunction, acute pulmonary hypertension or deep vein thrombosis in the lower limbs.

Ultrasound scanning protocol

Evaluation of patients with acute respiratory failure using the Bedside Lung Ultrasound in Emergency Protocol (BLUE protocol), is one of the best-known applications of LUS[37]. In the particular case of COVID-19, one of its main challenges lies in standardising the technique to allow comparisons between study groups.

In clinical practice – and especially in ICUs – certain specific scanning protocols have been designed to quantify the extent of lung involvement by COVID-19[29,38-40]. We highlight the proposal of Soldati *et al*[38], which delimits seven exploration

Table 3 Common ultrasound findings in coronavirus disease 2019

B pattern: Presence of multifocal and separated B-lines ("*waterfall sign*") or confluent B-lines ("*white lung*"). The distribution is predominantly posteroinferior and bilateral, and varies depending on the severity of the disease
Patchy involvement: Pathological areas of lung parenchyma alternating with well-aerated and preserved areas
Thickening or interruption of pleural line, and reduced pleural sliding
Small subpleural consolidations in any region of the lung, more common at bases. Less frequently, larger consolidations may be found, with or without dynamic air bronchogram
Decrease in blood flow (within doppler mode) related to subpleural consolidations
Small or absent pleural effusion

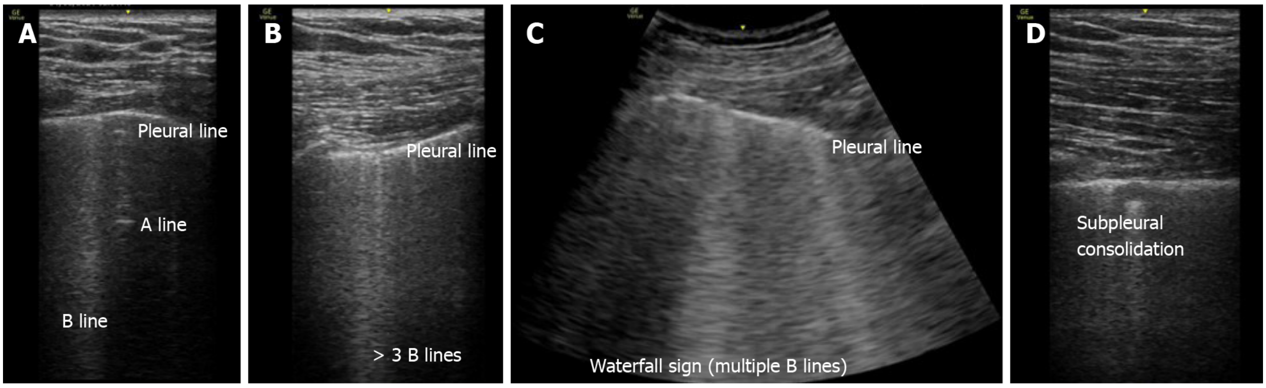

Figure 4 Images demonstrating the main changes in lung ultrasonography in coronavirus disease 2019 patients. A: Normal A-pattern with presence of 1 B line. B: Normal pleural line with presence of > 3 B lines. C: Irregular pleural line with coalescent B lines. D: Pleural involvement as sign of poor areation.

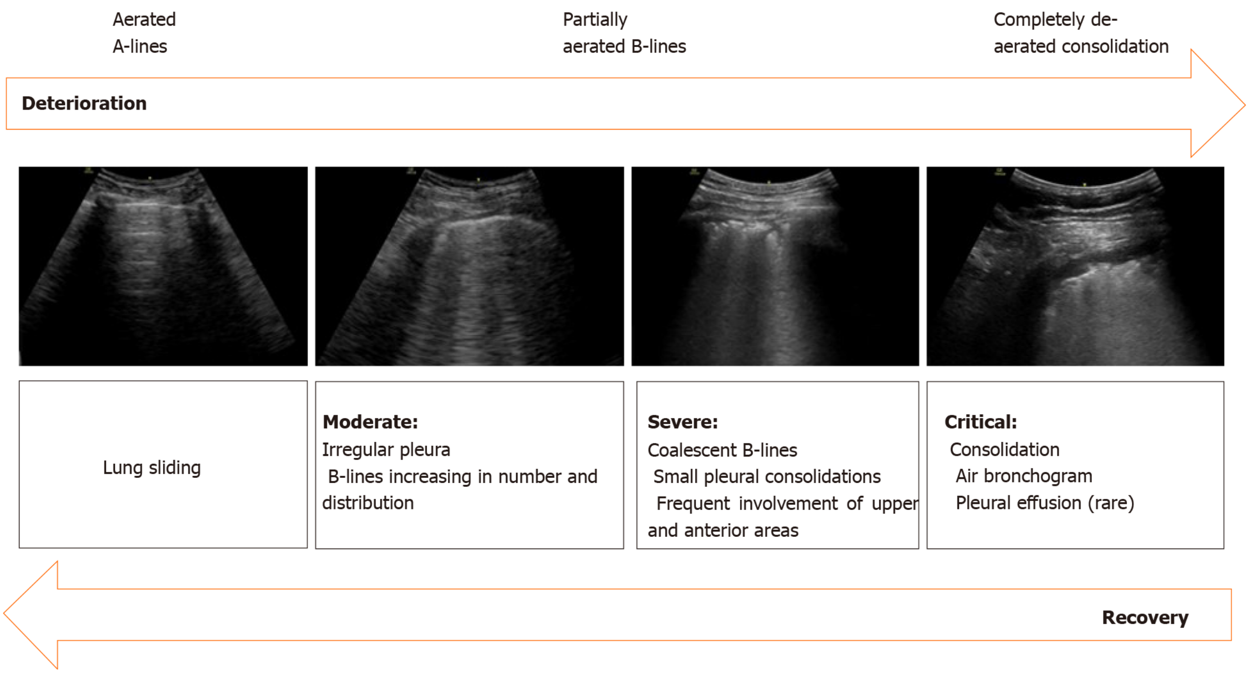

Figure 5 Sonographic characteristics of moderate, severe and critical pleural and parenchymal changes in patients with coronavirus disease 2019.

areas in each hemithorax, 14 zones in total. Each hemithorax is divided by three longitudinal lines – at the sternal, anterior and posterior axillary lines – and a transverse line at the nipple level, which separates a superior and an inferior area. Each one of the segments described receives a score between 0–3, according to the predominant findings in them, defining four different patterns (Table 4, Figure 4)[40].

At the end of the exploration, the score assigned to every explored area is accumulated, obtaining the final score. In the case of patterns B1 and B2, special attention must be paid to the pleural line, since the presence of pleural lesions is a severity sign that should be indicated by adding the letter ‘p’ to the score.

Ultimately, this scale allows the estimation of the extent of lung involvement in COVID-19 and provides clinical and prognostic information. Therefore, it could contribute to identifying those patients who require hospital admission, as well as to predict their response to certain therapies, such as prone positioning or mechanical ventilation. For example, the progressive reduction in the number of *B lines*, the reappearance of *A lines* or the regression of consolidations could suggest a favourable clinical evolution and support the decision to progress in the de-escalation of care.

A summary of the potential applications of LUS in COVID-19 pandemic is outlined below: (1) At triage: For risk stratification and initial screening of lung involvement in patients with suspected or confirmed SARS-CoV-2 infection; (2) In patients with symptoms consistent with COVID-19, but a negative nasopharyngeal swab (RT-PCR) and indeterminate chest X-ray: The presence of suggestive ultrasound findings could support the idea that the RT-PCR may represent a false-negative result; and (3) During hospital admission, to monitor the progression or regression of pulmonary lesions: Successive ultrasound explorations might result in accurate information that could be used to determine ventilation strategies and assess patients’ response to them. For example, those with posterolateral consolidations could benefit from early prone positioning[41,42], or lung aeration could be improved in those with coalescent *B lines* by titrating positive end-expiratory pressure (PEEP). In addition, in critically-ill patients – respiratory or hemodynamically unstable – LUS could play a remarkable role in the early detection of complications, including superimposed bacterial pneumonia and pneumothorax, and as a guide for clinical decisions.

Therefore, LUS is becoming an increasingly valuable diagnostic tool due to its high sensitivity, safety, immediacy and accuracy. On this basis, it may play a key role in the management of patients with COVID-19. However, its low specificity for this pathology does not allow clinicians to distinguish COVID-19 from other viral infections. Therefore, LUS images must be evaluated in conjunction with clinical and microbiological data.

ROLE OF CHEST CT SCAN IN THE EVALUATION OF COVID-19 PNEUMONIA

Chest CT scan is a key element in the management of SARS-CoV-2 infection. It allows the detection of distinctive pulmonary manifestations, establishes their severity and enables the follow-up of their progression, differentiating early stages from more advanced ones based on the radiological findings identified. However, its role as a screening tool in COVID-19 pneumonia has yet to be fully defined[43].

Recent studies concerning COVID-19 pneumonia propose that chest CT is a more sensitive, practical and rapid diagnostic technique compared to the RT-PCR test, especially in the early stages of the disease (Table 5). Ai *et al*[44] reported a sensitivity for chest CT of 97%, taking RT-PCR as a reference, compared to 59% of RT-PCR performed in patients with suspected SARS-CoV-2 infection. However, chest CT specificity was only 25%. Furthermore, a meta-analysis conducted by Kim *et al*[45] produced similar results, with a higher chest CT sensitivity than the one found for RT-PCR, 94% and 89%, respectively. However, a low specificity (37%) was encountered, which could be due to the fact that the nonspecific findings of COVID-19 pneumonia may overlap with those found in other viral pneumonias, so a high rate of false positives can be detected in chest CTs, especially in areas of low prevalence of the disease.

Supporting these results, the Society of Thoracic Radiology, the ACR and the Radiological Society of North America recommend avoiding using chest CT as a routine screening test in patients with suspected SARS-CoV-2 infection[46]. Instead it should be saved for the assessment of symptomatic patients or those with a negative RT-PCR but high clinical suspicion, as it can help to characterise the disease by detecting typical pulmonary manifestations[47].

Thus, chest CT findings suggesting viral pneumonia, accompanied by a typical clinical presentation and compatible epidemiological data, should strongly indicate SARS-CoV-2 infection even though the RT-PCR may be negative[48].

Table 4 Adapted from Vetrugno *et al*[39] proposal of lung ultrasonography score system in coronavirus disease 2019

Class	Score	Definition
A	0 point	Normal aeration pattern. Presence of *A lines*, pleural sliding, and ≤ 3 well-spaced *B lines*
B1	1 point	More than 3 *B lines* per intercostal space
B2	2 points	Confluent *B lines* (with or without small consolidations). This pattern corresponds to the presence of GGO on chest CT scan
C	3 points	Large consolidations, parenchymal hepatization (with or without air bronchogram)

CT: Computed tomography; GGO: Ground-glass opacity.

Table 5 Chest computed tomography and reverse transcription-polymerase chain reaction sensitivity in coronavirus disease 2019 pneumonia

Ref.	Number of patients	Symptoms	Positive RT-PCR	RT-PCR sensitivity	Chest CT abnormalities	Chest CT sensitivity
Fang *et al*[76], 2020	51	Fever/acute respiratory symptoms	36/51 patients	71%	50/51 patients	98%
Xie *et al*[48], 2020	167	Fever	162/167 patients	97%	160/167 patients	95.8%
Yang *et al*[77], 2020	149	Fever, cough and sputum	149/149	100%	132/149	88.6%
Ai *et al*[44], 2020	1014	–	601/1014	59%	888/1014	88%
Kim *et al*[45], 2020	7720	–	1336/1502	89%	5845/6218	94%

RT-PCR: Reverse transcription-polymerase chain reaction; CT: Computed tomography.

There are currently few works on the use of artificial intelligence in the diagnosis of SARS-CoV-2. Although this technique could be useful in diagnosing COVID-19 pneumonia, there is little evidence so far to recommend it as a routine diagnostic approach[49].

Chest CT imaging features of COVID-19

SARS-CoV-2 infection causes direct lung damage through the angiotensin-converting enzyme. Interstitial pneumonia with alveolar edema in the early stages and diffuse alveolar damage in the most severe stages are the underlying pathological mechanisms responsible for the typical radiological images of COVID-19 pneumonia and its rapid progression[50,51].

A wide range of radiological findings have been reported in the multiple published studies (Table 6); however, the images may differ depending on the evolutionary stage of the disease. The main and most frequent finding of COVID-19 pneumonia is the presence of GGOs, typically subpleural (Figure 6)[52,53]. GGOs are defined as areas of slightly increased density without obscuration of bronchial and vascular structures, caused by a partial filling of the alveolar spaces and interstitial thickening. In an investigation conducted by Chung *et al*[53] with 21 COVID-19 patients, GGOs – being the most characteristic radiological finding in the early stages of the disease – were found in 57% of cases[54]. In accordance with these results, Pan *et al*[55] predominantly observed subpleural GGOs at the onset of the disease, with the subsequent development of a 'crazy paving' pattern and consolidations at two weeks of evolution.

Regarding the distribution of the radiological images encountered, a retrospective study of 101 patients[56] classified them as either bilateal (82.2%), peripheral (87.1%) or multifocal (54.5%), principally involving the lower lobes (54.5%) of the patients. These results are broadly in line with other published studies. In a study conducted by Salehi *et al*[57], pulmonary changes were bilateral (87.5%), with a peripheral distribution (76.0%) and a predominantly multilobar (78.8%) and posterior (80.4%) pulmonary infiltration.

Table 6 Adapted from Carotti *et al*[57] average percentage of chest computed tomography manifestations of coronavirus disease 2019

Average percentage of chest computed tomography manifestations of coronavirus		
Ground-glass opacities	66%	+++++
Ground-glass opacities + consolidation	47%	++++
Consolidation	41%	++++
Interlobular septal thickening	53%	++++
Reticular pattern	27%	++
Crazy paving pattern	20%	++
Air bronchogram sign	50%	++++
Bronchial wall thickening	17%	++
Pleural effusion	10%	+
Nodules	15%	++
Reverse halo sign	3%	+
Lymphadenopathies	8%	+
Pericardial effusion	4%	+

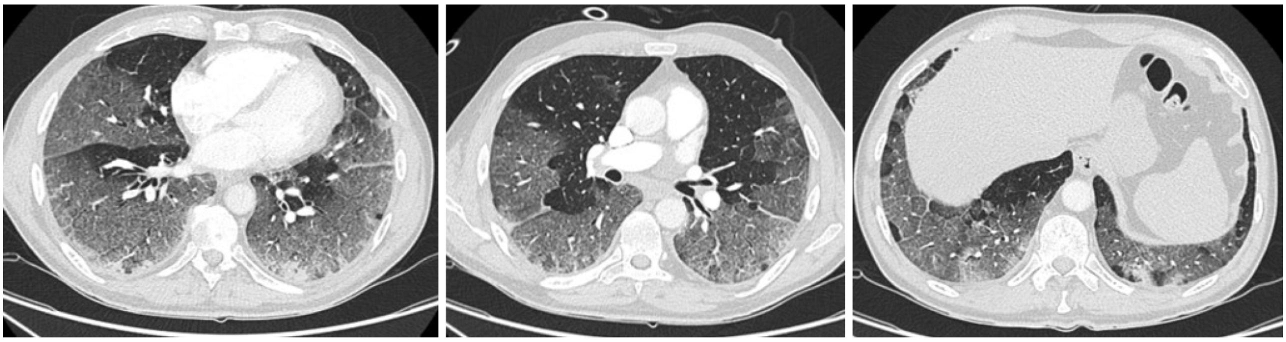

Figure 6 59-year-old man with no clinical background and confirmed severe acute respiratory syndrome coronavirus-2 infection. Chest computed tomography imaging with peripherally distributed bilateral and multilobar ground-glass opacities.

Consolidation images have been described as the second most prevalent finding, reported in 2%-63% of cases. The involvement may be multifocal, patchy, or segmental, with a subpleural or peribronchovascular distribution. The development of this consolidation pattern may be in relation to the progression of the disease and can either coexist alongside or replace GGOs between week one to three of the clinical course, which could alert to the severity of the disease[55,58] (Figure 7).

Recent investigations have reported 5%-36% of COVID-19 patients with a crazy paving pattern on their imaging studies. This pattern refers to the appearance of GGOs with superimposed interlobular and intralobular septal thickening. While not observed as frequently as GGOs and consolidation, this pattern may be a sign that the disease is reaching its peak of maximum severity[54], which is described by Pan *et al* [55] as occurring 10 d after the onset of symptoms.

Other findings, such as the reverse halo sign (11.0%), the air bronchogram sign (14%), pleural thickening (15.0%), pleural effusion (4.0%) and the appearance of lymphadenopathies (2.7%), have been less frequently described[59]. Bronchial wall thickening and the presence of extrapulmonary lesions suggest severe inflammation and are characteristic of critical COVID-19 pneumonia (Figure 8)[60].

A reticular pattern associated with bronchiolectasis and irregular thickening of the interlobular septa has been identified with the progression of the disease, usually after the second week of evolution (Figure 9). These interstitial changes suggest the development of fibrosis. Pulmonary fibrosis is a relatively common consequence of ARDS. Approximately 40% of patients diagnosed with COVID-19 pneumonia are believed to develop ARDS, 20% of them severe. Although long-term studies have shown the existence of persistent interstitial alterations in patients who have suffered

Figure 7 45-year-old woman with coronavirus disease 2019-confirmed pneumonia. Chest computed tomography imaging. A: Bilateral and patchy ground-glass opacities involving upper and lower lobes. B: Crazy paving pattern involving upper and lower lobes. C: Alveolar consolidation mainly involving the lower lobes, with fibrous stripes associated.

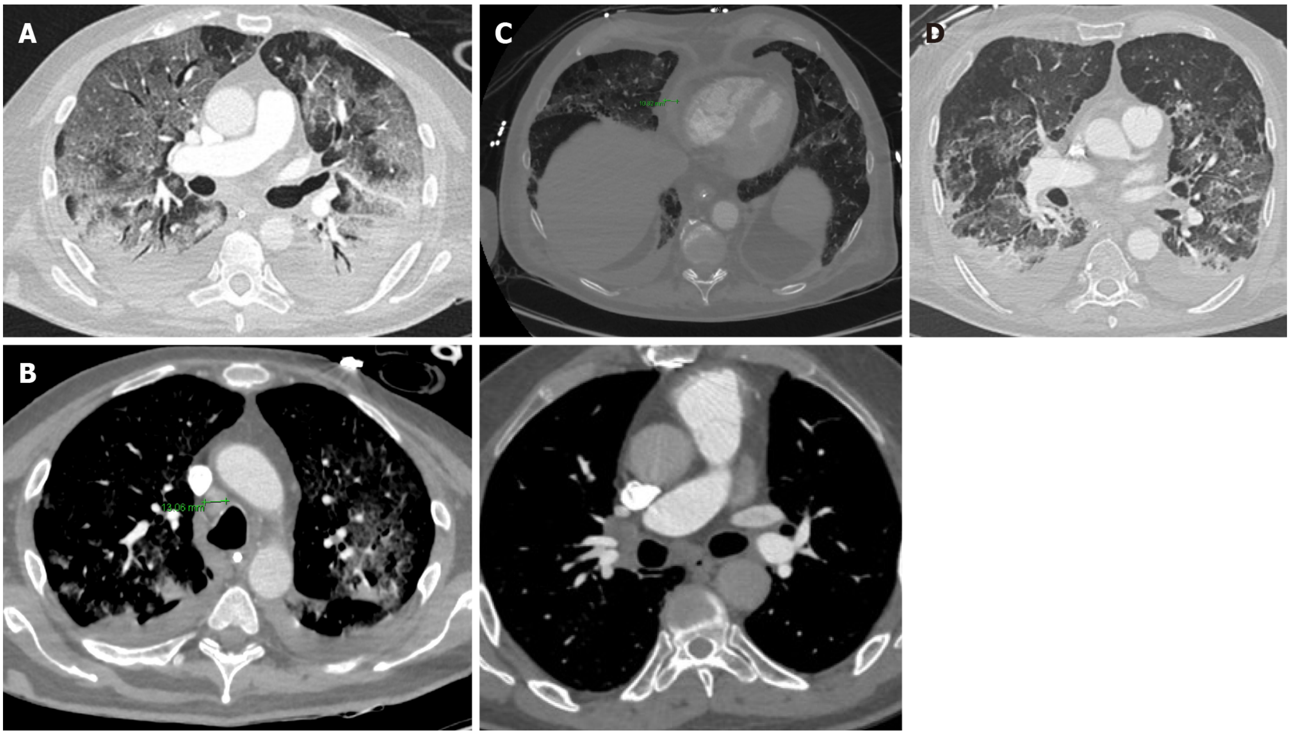

Figure 8 Unusual chest computed tomography findings in coronavirus disease 2019 pneumonia. A: Air bronchogram sign; B: Right paratracheal lymphadenopathy (marked) and right hilar lymphadenopathy; C: Pericardial effusion; D: Pleural effusion.

pneumonia due to other coronaviruses genetically similar to SARS-CoV-2 – SARS-CoV and MERS-CoV, first identified in 2002 and 2012 respectively[61,62], – the natural history of COVID-19 pneumonia has not yet been fully defined. Therefore, it is too early to classify these pulmonary changes as irreversible fibrotic changes, meaning that future prospective studies are necessary to confirm these preliminary results.

FLUORODEOXYGLUCOSE-POSITRON EMISSION TOMOGRAPHY IN COVID-19

PET-CT imaging with fluorodeoxyglucose (FDG) is a relevant and well-established diagnostic tool in tumoral pathology; in combination with CT, it provides anatomical and functional information that facilitates the study of tumoral extension and the evaluation of therapeutic response. This technique has also recently been gaining a certain importance in inflammatory and infectious pathologies. However, it has not yet been validated in this field and its use is not routinely recommended[63].

Several studies have suggested that PET-CT may be useful to evaluate the immune response to viral infections and their progression[64,65], since FDG uptake increases in

Figure 9 Reticular pattern and fibrous stripes showing coronavirus disease 2019 pneumonia in evolution (> 2 wk after the onset of symptoms).

neutrophils, lymphocytes, activated macrophages and granulocytes where there is inflammation. Therefore, it enables the localisation of where the immune response starts and how it develops.

Some authors have used PET-CT in animal models to study the development of viral infections, including MERS-CoV, H1N1, and HIV[66-68]. After exposure to the virus, in the absence of symptoms or abnormalities in chest CT scans, PET-CT is able to detect increased cellular metabolism in the lymph node stations directly involved in the lymphatic drainage of the lung tissue: the mediastinal and axillary nodes[66]. Furthermore, this increase in FDG uptake is observed before massive viral replication occurs[68]; therefore, PET-CT could have a significant utility in early stages of infection.

In line with other inflammatory processes, the lung areas affected by COVID-19 show an increased FDG uptake (Figure 10)[69]. It has been postulated that there could be a correlation between greater FDG uptake and a slower progression towards improvement, as well as a higher erythrocyte sedimentation rate[70]. Various studies – which compare the findings of PET-CT and chest CT scans in COVID-19 patients – have also reported that despite the absence of lymphadenopathy in CT, PET-CT does detect an increased FDG uptake at the mediastinal and subclavicular lymph nodes[70-73]. Additionally, in some patients infected by SARS-CoV-2, mild inflammatory activity has been observed in the spleen and bone marrow, possibly in relation to a systemic inflammatory state. Finally, Lutje *et al*[74] proposed that PET-CT with FDG might help in detecting changes in other organs, including the heart, kidneys and gastrointestinal tract. However, all of the data published so far agree that the inflammatory process triggered by COVID-19 has a particular tropism for the lower respiratory tract.

Preliminary studies have suggested that there is a certain correlation between the metabolic information provided by PET-CT and the degree of ventilation in different areas of the lung[75]. The collected data indicate that poorly ventilated areas of lung parenchyma show a greater FDG uptake than non-ventilated areas. This might mean that, within inflammatory processes, the better ventilated areas of the lung probably present higher infiltration by inflammatory cells[76].

PET-CT is not recommended as an initial test for diagnosing SARS-CoV-2 infection, as it involves greater irradiation to the patient than chest X-ray or chest CT scan, and the image acquisition periods are longer. Nonetheless, the structural and metabolic image that it provides could have an application in COVID-19 in the following situations[77]: (1) As a diagnostic tool for differential diagnosis in asymptomatic patients and in already diagnosed patients with a normal CT scan; (2) For monitoring responses to therapy, in combination with chest CT scan; (3) As a potential prognostic factor in the recovery stage of the disease; and (4) To evaluate extrapulmonary systemic involvement.

In conclusion, the studies published to date on the potential role of PET-CT in COVID-19 are limited. However, the existing data suggest that it may provide

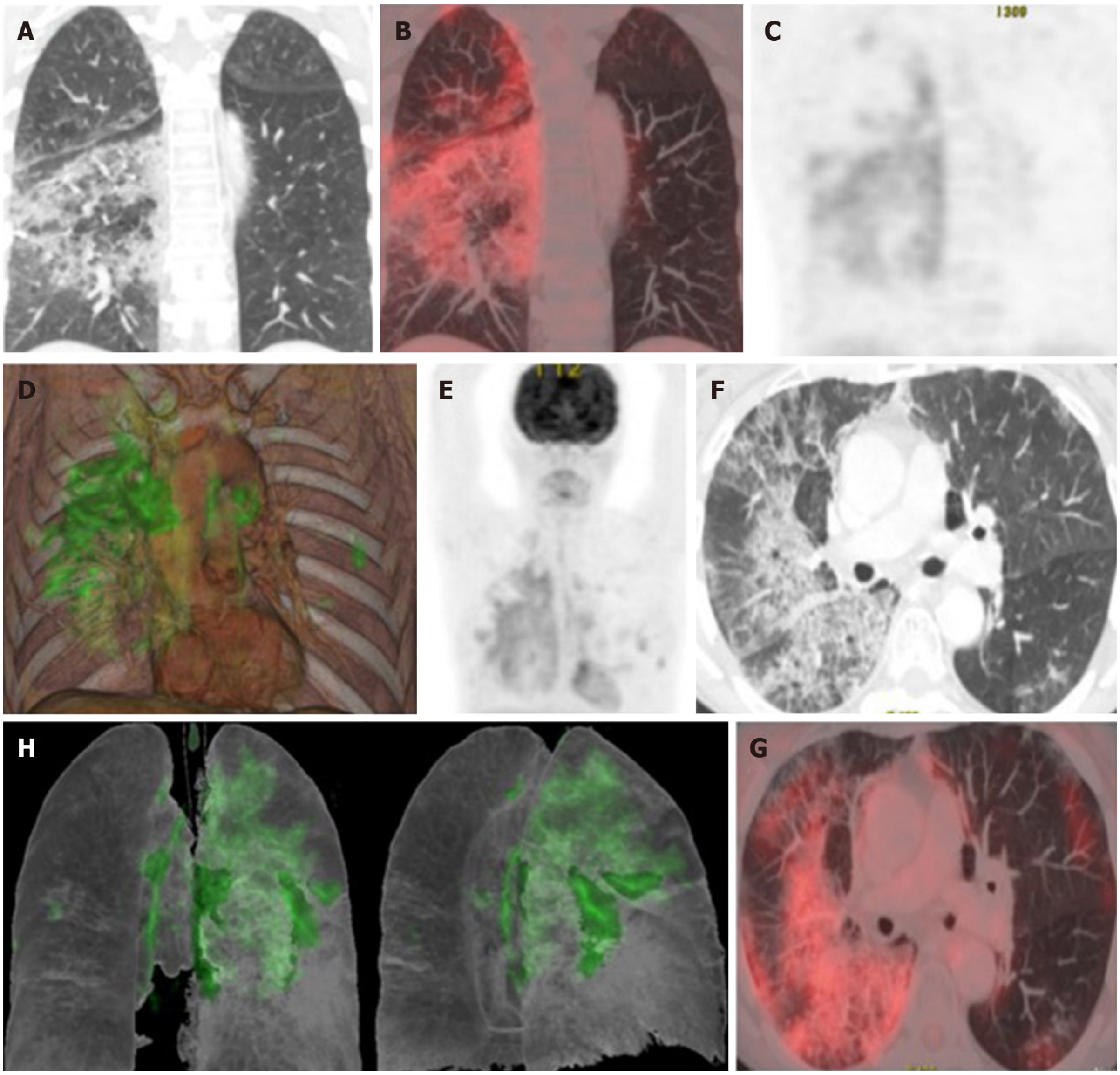

Figure 10 Taken from Landete *et al*[12], A 65-year-old patient with a history of invasive lepidic-predominant adenocarcinoma (stage pT1bNxM0) treated with surgery, chemotherapy and radiotherapy. A: Coronal computed tomography (CT) showing the crazy paving pattern with a markedly asymmetric bilateral distribution, mainly affecting the right side. B: Positron emission tomography-CT (PET-CT) coronal section. C: Metabolic PET. D: Volume rendering 3D PET-CT. E: MIP, PET. Images B–E reveal an increased cellular activity [standard uptake value (SUV) 4-6] related to the associated inflammatory process and a PET-CT pattern of bilateral coronavirus disease 2019 (COVID-19) with viral pneumonitis, predominantly right-sided. F: Axial CT showing crazy paving pattern with a bilateral, yet markedly asymmetric distribution, predominant right-sided. G and H: Axial section and 3D volume rendering from PET-CT metabolic imaging revealing increased cellular activity (SUV 4-6) related to the associated inflammatory process. PET-CT pattern of bilateral, predominantly right-sided, COVID-19 viral pneumonitis. Citation: Landete P, Quezada Loaiza CA, Aldave-Orzaiz B, Muñiz SH, Maldonado A, Zamora E, Sam Cerna AC, Del Cerro E, Alonso RC, Couñago F. Clinical features and radiological manifestations of COVID-19 disease. *World J Radiol* 2020; 12(11): 247-260. Copyright ©The Author(s) 2020. Published by Baishideng Publishing Group Inc[12]".

valuable information – complementary to the other imaging tests mentioned in this review – which helps to understand the pathophysiology of SARS-CoV-2 infection, define therapeutic strategies and assess the response to them.

CONCLUSION

Chest X-ray and CT play an important role in detecting abnormal lung changes, being the main imaging tests used to diagnose COVID-19 pneumonia. Other radiological modalities, such as lung ultrasonography and PET-CT, can provide further information for initial assessment and follow-up treatment response. Moreover, as we move through the pandemic, we believe that radiological findings of COVID-19 will be further explored, helping in determining diagnostic imaging features and guiding treatment.

REFERENCES

1 **Sohrabi C**, Alsafi Z, O'Neill N, Khan M, Kerwan A, Al-Jabir A, Iosifidis C, Agha R. World Health Organization declares global emergency: A review of the 2019 novel coronavirus (COVID-19). *Int J Surg* 2020; **76**: 71-76 [PMID: 32112977 DOI: 10.1016/j.ijsu.2020.02.034]

2 **Udugama B**, Kadhiresan P, Kozlowski HN, Malekjahani A, Osborne M, Li VYC, Chen H, Mubareka S, Gubbay JB, Chan WCW. Diagnosing COVID-19: The Disease and Tools for Detection. *ACS Nano* 2020; **14**: 3822-3835 [PMID: 32223179 DOI: 10.1021/acsnano.0c02624]

3 **World Health Organization**. COVID-19 Weekly epidemiological update-8 December 2020. [cited 20 January 2021] Available from: https://www.who.int/publications/m/item/weekly-epidemiological-update-8-december-2020

4 **Pascarella G**, Strumia A, Piliego C, Bruno F, Del Buono R, Costa F, Scarlata S, Agrò FE. COVID-19 diagnosis and management: a comprehensive review. *J Intern Med* 2020; **288**: 192-206 [PMID: 32348588 DOI: 10.1111/joim.13091]

5 **Aljondi R**, Alghamdi S. Diagnostic Value of Imaging Modalities for COVID-19: Scoping Review. *J Med Internet Res* 2020; **22**: e19673 [PMID: 32716893 DOI: 10.2196/19673]

6 **Wiersinga WJ**, Rhodes A, Cheng AC, Peacock SJ, Prescott HC. Pathophysiology, Transmission, Diagnosis, and Treatment of Coronavirus Disease 2019 (COVID-19): A Review. *JAMA* 2020; **324**: 782-793 [PMID: 32648899 DOI: 10.1001/jama.2020.12839]

7 **Araujo-Filho JAB**, Sawamura MVY, Costa AN, Cerri GG, Nomura CH. COVID-19 pneumonia: what is the role of imaging in diagnosis? *J Bras Pneumol* 2020; **46**: e20200114 [PMID: 32236303 DOI: 10.36416/1806-3756/e20200114]

8 **Gandhi D**, Ahuja K, Grover H, Sharma P, Solanki S, Gupta N, Patel L. Review of X-ray and computed tomography scan findings with a promising role of point of care ultrasound in COVID-19 pandemic. *World J Radiol* 2020; **12**: 195-203 [PMID: 33033574 DOI: 10.4329/wjr.v12.i9.195]

9 **Rubin GD**, Ryerson CJ, Haramati LB, Sverzellati N, Kanne JP, Raoof S, Schluger NW, Volpi A, Yim JJ, Martin IBK, Anderson DJ, Kong C, Altes T, Bush A, Desai SR, Goldin J, Goo JM, Humbert M, Inoue Y, Kauczor HU, Luo F, Mazzone PJ, Prokop M, Remy-Jardin M, Richeldi L, Schaefer-Prokop CM, Tomiyama N, Wells AU, Leung AN. The Role of Chest Imaging in Patient Management During the COVID-19 Pandemic: A Multinational Consensus Statement From the Fleischner Society. *Chest* 2020; **158**: 106-116 [PMID: 32275978 DOI: 10.1016/j.chest.2020.04.003]

10 **Farias LPG**, Fonseca EKUN, Strabelli DG, Loureiro BMC, Neves YCS, Rodrigues TP, Chate RC, Nomura CH, Sawamura MVY, Cerri GG. Imaging findings in COVID-19 pneumonia. *Clinics (Sao Paulo)* 2020; **75**: e2027 [PMID: 32578826 DOI: 10.6061/clinics/2020/e2027]

11 **Revel MP**, Parkar AP, Prosch H, Silva M, Sverzellati N, Gleeson F, Brady A; European Society of Radiology (ESR) and the European Society of Thoracic Imaging (ESTI). COVID-19 patients and the radiology department - advice from the European Society of Radiology (ESR) and the European Society of Thoracic Imaging (ESTI). *Eur Radiol* 2020; **30**: 4903-4909 [PMID: 32314058 DOI: 10.1007/s00330-020-06865-y]

12 **Landete P**, Quezada Loaiza CA, Aldave-Orzaiz B, Muñiz SH, Maldonado A, Zamora E, Sam Cerna AC, Del Cerro E, Alonso RC, Couñago F. Clinical features and radiological manifestations of COVID-19 disease. *World J Radiol* 2020; **12**: 247-260 [PMID: 33362916 DOI: 10.4329/wjr.v12.i11.247]

13 **Wong HYF**, Lam HYS, Fong AH, Leung ST, Chin TW, Lo CSY, Lui MM, Lee JCY, Chiu KW, Chung TW, Lee EYP, Wan EYF, Hung IFN, Lam TPW, Kuo MD, Ng MY. Frequency and Distribution of Chest Radiographic Findings in Patients Positive for COVID-19. *Radiology* 2020; **296**: E72-E78 [PMID: 32216717 DOI: 10.1148/radiol.2020201160]

14 **Ng MY**, Lee EYP, Yang J, Yang F, Li X, Wang H, Lui MM, Lo CS, Leung B, Khong PL, Hui CK, Yuen KY, Kuo MD. Imaging Profile of the COVID-19 Infection: Radiologic Findings and Literature Review. *Radiol Cardiothorac Imaging* 2020; **2**: e200034 [PMID: 33778547 DOI: 10.1148/ryct.2020200034]

15 **Kim ES**, Chin BS, Kang CK, Kim NJ, Kang YM, Choi JP, Oh DH, Kim JH, Koh B, Kim SE, Yun NR, Lee JH, Kim JY, Kim Y, Bang JH, Song KH, Kim HB, Chung KH, Oh MD; Korea National Committee for Clinical Management of COVID-19. Clinical Course and Outcomes of Patients with Severe Acute Respiratory Syndrome Coronavirus 2 Infection: a Preliminary Report of the First 28 Patients from the Korean Cohort Study on COVID-19. *J Korean Med Sci* 2020; **35**: e142 [PMID: 32242348 DOI: 10.3346/jkms.2020.35.e142]

16 **Chen N**, Zhou M, Dong X, Qu J, Gong F, Han Y, Qiu Y, Wang J, Liu Y, Wei Y, Xia J, Yu T, Zhang X, Zhang L. Epidemiological and clinical characteristics of 99 cases of 2019 novel coronavirus pneumonia in Wuhan, China: a descriptive study. *Lancet* 2020; **395**: 507-513 [PMID: 32007143 DOI: 10.1016/S0140-6736(20)30211-7]

17 **Cellina M**, Panzeri M, Oliva G. Chest Radiography Features Help to Predict a Favorable Outcome in Patients with Coronavirus Disease 2019. *Radiology* 2020; **297**: E238 [PMID: 32484419 DOI: 10.1148/radiol.2020202326]

18 **Jacobi A**, Chung M, Bernheim A, Eber C. Portable chest X-ray in coronavirus disease-19 (COVID-

19): A pictorial review. *Clin Imaging* 2020; **64**: 35-42 [PMID: 32302927 DOI: 10.1016/j.clinimag.2020.04.001]

19 **Lomoro P**, Verde F, Zerboni F, Simonetti I, Borghi C, Fachinetti C, Natalizi A, Martegani A. COVID-19 pneumonia manifestations at the admission on chest ultrasound, radiographs, and CT: single-center study and comprehensive radiologic literature review. *Eur J Radiol Open* 2020; **7**: 100231 [PMID: 32289051 DOI: 10.1016/j.ejro.2020.100231]

20 **Lemmers DHL**, Abu Hilal M, Bnà C, Prezioso C, Cavallo E, Nencini N, Crisci S, Fusina F, Natalini G. Pneumomediastinum and subcutaneous emphysema in COVID-19: barotrauma or lung frailty? *ERJ Open Res* 2020; **6** [PMID: 33257914 DOI: 10.1183/23120541.00385-2020]

21 **Chen SG**, Chen JY, Yang YP, Chien CS, Wang ML, Lin LT. Use of radiographic features in COVID-19 diagnosis: Challenges and perspectives. *J Chin Med Assoc* 2020; **83**: 644-647 [PMID: 32349032 DOI: 10.1097/JCMA.0000000000000336]

22 **Zhang YK**, Li J, Yang JP, Zhan Y, Chen J. Lung ultrasonography for the diagnosis of 11 patients with acute respiratory distress syndrome due to bird flu H7N9 infection. *Virol J* 2015; **12**: 176 [PMID: 26503117 DOI: 10.1186/s12985-015-0406-1]

23 **Tsai NW**, Ngai CW, Mok KL, Tsung JW. Lung ultrasound imaging in avian influenza A (H7N9) respiratory failure. *Crit Ultrasound J* 2014; **6**: 6 [PMID: 24949191 DOI: 10.1186/2036-7902-6-6]

24 **Volpicelli G**, Elbarbary M, Blaivas M, Lichtenstein DA, Mathis G, Kirkpatrick AW, Melniker L, Gargani L, Noble VE, Via G, Dean A, Tsung JW, Soldati G, Copetti R, Bouhemad B, Reissig A, Agricola E, Rouby JJ, Arbelot C, Liteplo A, Sargsyan A, Silva F, Hoppmann R, Breitkreutz R, Seibel A, Neri L, Storti E, Petrovic T; International Liaison Committee on Lung Ultrasound (ILC-LUS) for International Consensus Conference on Lung Ultrasound (ICC-LUS). International evidence-based recommendations for point-of-care lung ultrasound. *Intensive Care Med* 2012; **38**: 577-591 [PMID: 22392031 DOI: 10.1007/s00134-012-2513-4]

25 **Mojoli F**, Bouhemad B, Mongodi S, Lichtenstein D. Lung Ultrasound for Critically Ill Patients. *Am J Respir Crit Care Med* 2019; **199**: 701-714 [PMID: 30372119 DOI: 10.1164/rccm.201802-0236CI]

26 **Alzahrani SA**, Al-Salamah MA, Al-Madani WH, Elbarbary MA. Systematic review and meta-analysis for the use of ultrasound versus radiology in diagnosing of pneumonia. *Crit Ultrasound J* 2017; **9**: 6 [PMID: 28244009 DOI: 10.1186/s13089-017-0059-y]

27 **Tung-Chen Y**, Martí de Gracia M, Díez-Tascón A, Alonso-González R, Agudo-Fernández S, Parra-Gordo ML, Ossaba-Vélez S, Rodríguez-Fuertes P, Llamas-Fuentes R. Correlation between Chest Computed Tomography and Lung Ultrasonography in Patients with Coronavirus Disease 2019 (COVID-19). *Ultrasound Med Biol* 2020; **46**: 2918-2926 [PMID: 32771222 DOI: 10.1016/j.ultrasmedbio.2020.07.003]

28 **Poggiali E**, Dacrema A, Bastoni D, Tinelli V, Demichele E, Mateo Ramos P, Marcianò T, Silva M, Vercelli A, Magnacavallo A. Can Lung US Help Critical Care Clinicians in the Early Diagnosis of Novel Coronavirus (COVID-19) Pneumonia? *Radiology* 2020; **295**: E6 [PMID: 32167853 DOI: 10.1148/radiol.2020200847]

29 **Huang Y**, Wang S, Liu Y, Zhang Y, Zheng C, Zheng Y, Zhang C, Min W, Yu M, Hu M. A Preliminary Study on the Ultrasonic Manifestations of Peripulmonary Lesions of Non-Critical Novel Coronavirus Pneumonia (COVID-19) (February 26, 2020). [DOI: 10.2139/ssrn.3544750]

30 **Nouvenne A**, Zani MD, Milanese G, Parise A, Baciarello M, Bignami EG, Odone A, Sverzellati N, Meschi T, Ticinesi A. Lung Ultrasound in COVID-19 Pneumonia: Correlations with Chest CT on Hospital admission. *Respiration* 2020; **99**: 617-624 [PMID: 32570265 DOI: 10.1159/000509223]

31 **Peng QY**, Wang XT, Zhang LN; Chinese Critical Care Ultrasound Study Group (CCUSG). Findings of lung ultrasonography of novel corona virus pneumonia during the 2019-2020 epidemic. *Intensive Care Med* 2020; **46**: 849-850 [PMID: 32166346 DOI: 10.1007/s00134-020-05996-6]

32 **Volpicelli G**, Gargani L. Sonographic signs and patterns of COVID-19 pneumonia. *Ultrasound J* 2020; **12**: 22 [PMID: 32318891 DOI: 10.1186/s13089-020-00171-w]

33 **Millington SJ**, Koenig S, Mayo P, Volpicelli G. Lung Ultrasound for Patients With Coronavirus Disease 2019 Pulmonary Disease. *Chest* 2021; **159**: 205-211 [PMID: 32835709 DOI: 10.1016/j.chest.2020.08.2054]

34 **Gattinoni L**, Chiumello D, Caironi P, Busana M, Romitti F, Brazzi L, Camporota L. COVID-19 pneumonia: different respiratory treatments for different phenotypes? *Intensive Care Med* 2020; **46**: 1099-1102 [PMID: 32291463 DOI: 10.1007/s00134-020-06033-2]

35 **Volpicelli G**, Lamorte A, Villén T. What's new in lung ultrasound during the COVID-19 pandemic. *Intensive Care Med* 2020; **46**: 1445-1448 [PMID: 32367169 DOI: 10.1007/s00134-020-06048-9]

36 **Smith MJ**, Hayward SA, Innes SM, Miller ASC. Point-of-care lung ultrasound in patients with COVID-19 - a narrative review. *Anaesthesia* 2020; **75**: 1096-1104 [PMID: 32275766 DOI: 10.1111/anae.15082]

37 **Lichtenstein DA**. BLUE-protocol and FALLS-protocol: two applications of lung ultrasound in the critically ill. *Chest* 2015; **147**: 1659-1670 [PMID: 26033127 DOI: 10.1378/chest.14-1313]

38 **Soldati G**, Smargiassi A, Inchingolo R, Buonsenso D, Perrone T, Briganti DF, Perlini S, Torri E, Mariani A, Mossolani EE, Tursi F, Mento F, Demi L. Proposal for International Standardization of the Use of Lung Ultrasound for Patients With COVID-19: A Simple, Quantitative, Reproducible Method. *J Ultrasound Med* 2020; **39**: 1413-1419 [PMID: 32227492 DOI: 10.1002/jum.15285]

39 **Vetrugno L**, Bove T, Orso D, Barbariol F, Bassi F, Boero E, Ferrari G, Kong R. Our Italian experience using lung ultrasound for identification, grading and serial follow-up of severity of lung involvement for management of patients with COVID-19. *Echocardiography* 2020; **37**: 625-627

[PMID: 32239532 DOI: 10.1111/echo.14664]
40 **Istvan-Adorjan S**, Ágoston G, Varga A, Cotoi OS, Frigy A. Pathophysiological background and clinical practice of lung ultrasound in COVID-19 patients: A short review. *Anatol J Cardiol* 2020; **24**: 76-80 [PMID: 32749247 DOI: 10.14744/AnatolJCardiol.2020.33645]
41 **Prat G**, Guinard S, Bizien N, Nowak E, Tonnelier JM, Alavi Z, Renault A, Boles JM, L'Her E. Can lung ultrasonography predict prone positioning response in acute respiratory distress syndrome patients? *J Crit Care* 2016; **32**: 36-41 [PMID: 26806842 DOI: 10.1016/j.jcrc.2015.12.015]
42 **Wang XT**, Ding X, Zhang HM, Chen H, Su LX, Liu DW; Chinese Critical Ultrasound Study Group (CCUSG). Lung ultrasound can be used to predict the potential of prone positioning and assess prognosis in patients with acute respiratory distress syndrome. *Crit Care* 2016; **20**: 385 [PMID: 27899151 DOI: 10.1186/s13054-016-1558-0]
43 **Sun Z**, Zhang N, Li Y, Xu X. A systematic review of chest imaging findings in COVID-19. *Quant Imaging Med Surg* 2020; **10**: 1058-1079 [PMID: 32489929 DOI: 10.21037/qims-20-564]
44 **Ai T**, Yang Z, Hou H, Zhan C, Chen C, Lv W, Tao Q, Sun Z, Xia L. Correlation of Chest CT and RT-PCR Testing for Coronavirus Disease 2019 (COVID-19) in China: A Report of 1014 Cases. *Radiology* 2020; **296**: E32-E40 [PMID: 32101510 DOI: 10.1148/radiol.2020200642]
45 **Kim H**, Hong H, Yoon SH. Diagnostic Performance of CT and Reverse Transcriptase Polymerase Chain Reaction for Coronavirus Disease 2019: A Meta-Analysis. *Radiology* 2020; **296**: E145-E155 [PMID: 32301646 DOI: 10.1148/radiol.2020201343]
46 **Simpson S**, Kay FU, Abbara S, Bhalla S, Chung JH, Chung M, Henry TS, Kanne JP, Kligerman S, Ko JP, Litt H. Radiological Society of North America Expert Consensus Statement on Reporting Chest CT Findings Related to COVID-19. Endorsed by the Society of Thoracic Radiology, the American College of Radiology, and RSNA - Secondary Publication. *J Thorac Imaging* 2020; **35**: 219-227 [PMID: 32324653 DOI: 10.1097/RTI.0000000000000524]
47 **Waller JV**, Kaur P, Tucker A, Lin KK, Diaz MJ, Henry TS, Hope M. Diagnostic Tools for Coronavirus Disease (COVID-19): Comparing CT and RT-PCR Viral Nucleic Acid Testing. *AJR Am J Roentgenol* 2020; **215**: 834-838 [PMID: 32412790 DOI: 10.2214/AJR.20.23418]
48 **Xie X**, Zhong Z, Zhao W, Zheng C, Wang F, Liu J. Chest CT for Typical Coronavirus Disease 2019 (COVID-19) Pneumonia: Relationship to Negative RT-PCR Testing. *Radiology* 2020; **296**: E41-E45 [PMID: 32049601 DOI: 10.1148/radiol.2020200343]
49 **Neri E**, Miele V, Coppola F, Grassi R. Use of CT and artificial intelligence in suspected or COVID-19 positive patients: statement of the Italian Society of Medical and Interventional Radiology. *Radiol Med* 2020; **125**: 505-508 [PMID: 32350794 DOI: 10.1007/s11547-020-01197-9]
50 **Li Y**, Xia L. Coronavirus Disease 2019 (COVID-19): Role of Chest CT in Diagnosis and Management. *AJR Am J Roentgenol* 2020; **214**: 1280-1286 [PMID: 32130038 DOI: 10.2214/AJR.20.22954]
51 **Li M**. Chest CT features and their role in COVID-19. *Radiol Infect Dis* 2020; **7**: 51-54 [PMID: 32309528 DOI: 10.1016/j.jrid.2020.04.001]
52 **Hani C**, Trieu NH, Saab I, Dangeard S, Bennani S, Chassagnon G, Revel MP. COVID-19 pneumonia: A review of typical CT findings and differential diagnosis. *Diagn Interv Imaging* 2020; **101**: 263-268 [PMID: 32291197 DOI: 10.1016/j.diii.2020.03.014]
53 **Chung M**, Bernheim A, Mei X, Zhang N, Huang M, Zeng X, Cui J, Xu W, Yang Y, Fayad ZA, Jacobi A, Li K, Li S, Shan H. CT Imaging Features of 2019 Novel Coronavirus (2019-nCoV). *Radiology* 2020; **295**: 202-207 [PMID: 32017661 DOI: 10.1148/radiol.2020200230]
54 **Ye Z**, Zhang Y, Wang Y, Huang Z, Song B. Chest CT manifestations of new coronavirus disease 2019 (COVID-19): a pictorial review. *Eur Radiol* 2020; **30**: 4381-4389 [PMID: 32193638 DOI: 10.1007/s00330-020-06801-0]
55 **Pan F**, Ye T, Sun P, Gui S, Liang B, Li L, Zheng D, Wang J, Hesketh RL, Yang L, Zheng C. Time Course of Lung Changes at Chest CT during Recovery from Coronavirus Disease 2019 (COVID-19). *Radiology* 2020; **295**: 715-721 [PMID: 32053470 DOI: 10.1148/radiol.2020200370]
56 **Zhao W**, Zhong Z, Xie X, Yu Q, Liu J. Relation Between Chest CT Findings and Clinical Conditions of Coronavirus Disease (COVID-19) Pneumonia: A Multicenter Study. *AJR Am J Roentgenol* 2020; **214**: 1072-1077 [PMID: 32125873 DOI: 10.2214/AJR.20.22976]
57 **Salehi S**, Abedi A, Balakrishnan S, Gholamrezanezhad A. Coronavirus Disease 2019 (COVID-19): A Systematic Review of Imaging Findings in 919 Patients. *AJR Am J Roentgenol* 2020; **215**: 87-93 [PMID: 32174129 DOI: 10.2214/AJR.20.23034]
58 **Carotti M**, Salaffi F, Sarzi-Puttini P, Agostini A, Borgheresi A, Minorati D, Galli M, Marotto D, Giovagnoni A. Chest CT features of coronavirus disease 2019 (COVID-19) pneumonia: key points for radiologists. *Radiol Med* 2020; **125**: 636-646 [PMID: 32500509 DOI: 10.1007/s11547-020-01237-4]
59 **Bai HX**, Hsieh B, Xiong Z, Halsey K, Choi JW, Tran TML, Pan I, Shi LB, Wang DC, Mei J, Jiang XL, Zeng QH, Egglin TK, Hu PF, Agarwal S, Xie FF, Li S, Healey T, Atalay MK, Liao WH. Performance of Radiologists in Differentiating COVID-19 from Non-COVID-19 Viral Pneumonia at Chest CT. *Radiology* 2020; **296**: E46-E54 [PMID: 32155105 DOI: 10.1148/radiol.2020200823]
60 **Li K**, Wu J, Wu F, Guo D, Chen L, Fang Z, Li C. The Clinical and Chest CT Features Associated With Severe and Critical COVID-19 Pneumonia. *Invest Radiol* 2020; **55**: 327-331 [PMID: 32118615 DOI: 10.1097/RLI.0000000000000672]
61 **Shi H**, Han X, Jiang N, Cao Y, Alwalid O, Gu J, Fan Y, Zheng C. Radiological findings from 81 patients with COVID-19 pneumonia in Wuhan, China: a descriptive study. *Lancet Infect Dis* 2020;

20: 425-434 [PMID: 32105637 DOI: 10.1016/S1473-3099(20)30086-4]

62 **Spagnolo P**, Balestro E, Aliberti S, Cocconcelli E, Biondini D, Casa GD, Sverzellati N, Maher TM. Pulmonary fibrosis secondary to COVID-19: a call to arms? *Lancet Respir Med* 2020; **8**: 750-752 [PMID: 32422177 DOI: 10.1016/S2213-2600(20)30222-8]

63 **Capitanio S**, Nordin AJ, Noraini AR, Rossetti C. PET/CT in nononcological lung diseases: current applications and future perspectives. *Eur Respir Rev* 2016; **25**: 247-258 [PMID: 27581824 DOI: 10.1183/16000617.0051-2016]

64 **de Prost N**, Tucci MR, Melo MF. Assessment of lung inflammation with 18F-FDG PET during acute lung injury. *AJR Am J Roentgenol* 2010; **195**: 292-300 [PMID: 20651183 DOI: 10.2214/AJR.10.4499]

65 **Brust D**, Polis M, Davey R, Hahn B, Bacharach S, Whatley M, Fauci AS, Carrasquillo JA. Fluorodeoxyglucose imaging in healthy subjects with HIV infection: impact of disease stage and therapy on pattern of nodal activation. *AIDS* 2006; **20**: 495-503 [PMID: 16470113 DOI: 10.1097/01.aids.0000210603.40267.29]

66 **Chefer S**, Thomasson D, Seidel J, Reba RC, Bohannon JK, Lackemeyer MG, Bartos C, Sayre PJ, Bollinger L, Hensley LE, Jahrling PB, Johnson RF. Modeling [(18)F]-FDG lymphoid tissue kinetics to characterize nonhuman primate immune response to Middle East respiratory syndrome-coronavirus aerosol challenge. *EJNMMI Res* 2015; **5**: 65 [PMID: 26573211 DOI: 10.1186/s13550-015-0143-x]

67 **Jonsson CB**, Camp JV, Wu A, Zheng H, Kraenzle JL, Biller AE, Vanover CD, Chu YK, Ng CK, Proctor M, Sherwood L, Steffen MC, Mollura DJ. Molecular imaging reveals a progressive pulmonary inflammation in lower airways in ferrets infected with 2009 H1N1 pandemic influenza virus. *PLoS One* 2012; **7**: e40094 [PMID: 22911695 DOI: 10.1371/journal.pone.0040094]

68 **Wallace M**, Pyzalski R, Horejsh D, Brown C, Djavani M, Lu Y, Hanson JM, Mitchen JL, Perlman SB, Pauza CD. Whole body positron emission tomography imaging of activated lymphoid tissues during acute simian-human immunodeficiency virus 89.6PD infection in rhesus macaques. *Virology* 2000; **274**: 255-261 [PMID: 10964769 DOI: 10.1006/viro.2000.0479]

69 **Dietz M**, Chironi G, Claessens YE, Farhad RL, Rouquette I, Serrano B, Nataf V, Hugonnet F, Paulmier B, Berthier F, Keita-Perse O, Giammarile F, Perrin C, Faraggi M; MONACOVID Group. COVID-19 pneumonia: relationship between inflammation assessed by whole-body FDG PET/CT and short-term clinical outcome. *Eur J Nucl Med Mol Imaging* 2021; **48**: 260-268 [PMID: 32712702 DOI: 10.1007/s00259-020-04968-8]

70 **Qin C**, Liu F, Yen TC, Lan X. ^{18}F-FDG PET/CT findings of COVID-19: a series of four highly suspected cases. *Eur J Nucl Med Mol Imaging* 2020; **47**: 1281-1286 [PMID: 32088847 DOI: 10.1007/s00259-020-04734-w]

71 **Setti L**, Kirienko M, Dalto SC, Bonacina M, Bombardieri E. FDG-PET/CT findings highly suspicious for COVID-19 in an Italian case series of asymptomatic patients. *Eur J Nucl Med Mol Imaging* 2020; **47**: 1649-1656 [PMID: 32342191 DOI: 10.1007/s00259-020-04819-6]

72 **Zou S**, Zhu X. FDG PET/CT of COVID-19. *Radiology* 2020; **296**: E118 [PMID: 32142399 DOI: 10.1148/radiol.2020200770]

73 **Polverari G**, Arena V, Ceci F, Pelosi E, Ianniello A, Poli E, Sandri A, Penna D. ^{18}F-Fluorodeoxyglucose Uptake in Patient With Asymptomatic Severe Acute Respiratory Syndrome Coronavirus 2 (Coronavirus Disease 2019) Referred to Positron Emission Tomography/Computed Tomography for NSCLC Restaging. *J Thorac Oncol* 2020; **15**: 1078-1080 [PMID: 32243920 DOI: 10.1016/j.jtho.2020.03.022]

74 **Lütje S**, Marinova M, Kütting D, Attenberger U, Essler M, Bundschuh RA. Nuclear medicine in SARS-CoV-2 pandemia: 18F-FDG-PET/CT to visualize COVID-19. *Nuklearmedizin* 2020; **59**: 276-280 [PMID: 32259853 DOI: 10.1055/a-1152-2341]

75 **Bellani G**, Messa C, Guerra L, Spagnolli E, Foti G, Patroniti N, Fumagalli R, Musch G, Fazio F, Pesenti A. Lungs of patients with acute respiratory distress syndrome show diffuse inflammation in normally aerated regions: a [18F]-fluoro-2-deoxy-D-glucose PET/CT study. *Crit Care Med* 2009; **37**: 2216-2222 [PMID: 19487931 DOI: 10.1097/CCM.0b013e3181aab31f]

76 **Fang Y**, Zhang H, Xie J, Lin M, Ying L, Pang P, Ji W. Sensitivity of Chest CT for COVID-19: Comparison to RT-PCR. *Radiology* 2020; **296**: E115-E117 [PMID: 32073353 DOI: 10.1148/radiol.2020200432]

77 **Yang W**, Cao Q, Qin L, Wang X, Cheng Z, Pan A, Dai J, Sun Q, Zhao F, Qu J, Yan F. Clinical characteristics and imaging manifestations of the 2019 novel coronavirus disease (COVID-19):A multi-center study in Wenzhou city, Zhejiang, China. *J Infect* 2020; **80**: 388-393 [PMID: 32112884 DOI: 10.1016/j.jinf.2020.02.016]

World Journal of Radiology

Submit a Manuscript: https://www.f6publishing.com

World J Radiol 2021 October 28; 13(10): 344-353

DOI: 10.4329/wjr.v13.i10.344

ISSN 1949-8470 (online)

ORIGINAL ARTICLE

Prospective Study

Shoulder adhesive capsulitis in cancer patients undergoing positron emission tomography - computed tomography and the association with shoulder pain

Daichi Hayashi, Elaine Gould, Robert Shroyer, Eric van Staalduinen, Jie Yang, Musa Mufti, Mingqian Huang

ORCID number: Daichi Hayashi 0000-0002-2067-5780; Elaine Gould 0000-0002-2674-1785; Robert Shroyer 0000-0002-2493-1710; Eric van Staalduinen 0000-0001-9786-2712; Jie Yang 0000-0003-3469-5931; Musa Mufti 0000-0002-4958-6298; Mingqian Huang 0000-0002-5734-0191.

Author contributions: Hayashi D, Gould E and Huang M designed the research study; Hayashi D, Gould E, Shroyer R, van Staalduinen E, Mufti M and Huang M performed the research including data collection and electronic medical record review; Gould E, Shroyer R and Huang M interpreted positron emission tomography - computed tomography images; Yang J performed the statistical analyses; Hayashi D analyzed results and wrote the manuscript; all authors have read, edited and approved the final manuscript.

Institutional review board statement: Our prospective study received Institutional Review Board approval at our institution (Protocol# 2015-3396-R2).

Clinical trial registration statement: Our study is not a clinical trial. Therefore, there is no Clinical Trial

Daichi Hayashi, Elaine Gould, Robert Shroyer, Eric van Staalduinen, Musa Mufti, Mingqian Huang, Department of Radiology, State University of New York at Stony Brook, Stony Brook, NY 11794, United States

Jie Yang, Department of Family, Population and Preventive Medicine, Stony Brook Medicine, Stony Brook, NY 11794, United States

Corresponding author: Daichi Hayashi, MD, PhD, Associate Professor, Department of Radiology, State University of New York at Stony Brook, HSC Level 4, Room 120, Stony Brook, NY 11794, United States. daichi.hayashi@stonybrookmedicine.edu

Abstract

BACKGROUND

Adhesive capsulitis is a relatively common condition that can develop in cancer patients during treatment. Positron emission tomography - computed tomography (PET-CT) is routinely performed as a follow-up study in cancer patients after therapy. Being aware of PET-CT findings to suggest shoulder adhesive capsulitis may help to alert clinicians for the diagnosis of unsuspected shoulder capsulitis.

AIM

To assess the association of shoulder adhesive capsulitis with cancer/therapy type and symptoms in cancer patients undergoing PET-CT.

METHODS

Our prospective study received Institutional Review Board approval. Written informed consent was obtained from all patients, who answered a questionnaire regarding shoulder pain/stiffness at the time of PET-CT study, between March 2015 and April 2019. Patients with advanced glenohumeral arthrosis, metastatic disease or other mass in the shoulder, or shoulder arthroplasty were excluded. Patterns of shoulder capsule 18F-fluorodeoxyglucose (FDG) uptake were noted. Standard Uptake Value (SUV)max and SUVmean values were measured at rotator interval (RI) and deltoid muscle in bilateral shoulders. Normalized SUV (SUV of RI/SUV of deltoid muscle) was also calculated. We assessed if SUV values are different between symptomatic and asymptomatic patients in both shoulders. Covariates were age, gender, and therapy type (surgery, chemotherapy, radi-

Registration Statement applicable to this submission.

Informed consent statement: Written informed consent was obtained from all patients.

Conflict-of-interest statement: All authors have nothing to disclose.

Data sharing statement: Patient data are not available for sharing for protection of patient confidentiality and anonymity. No additional data are available.

CONSORT 2010 statement: The authors have read the STROBE Statement—checklist of items, and the manuscript was prepared and revised according to the STROBE Statement—checklist of items.

Manuscript source: Unsolicited manuscript

Specialty type: Radiology, Nuclear Medicine and Medical Imaging

Country/Territory of origin: United States

Peer-review report's scientific quality classification

Grade A (Excellent): 0
Grade B (Very good): 0
Grade C (Good): C
Grade D (Fair): 0
Grade E (Poor): 0

Received: March 13, 2021
Peer-review started: March 13, 2021
First decision: July 31, 2021
Revised: August 3, 2021
Accepted: September 14, 2021

ation). Wilcoxon rank sum tests were used to compare unadjusted marginal differences for age, SUV measurements between symptomatic and asymptomatic patients. Multiple linear regression models were used to examine the relationship between right or left shoulder SUV measurements and symptom status, after adjusting for covariates. Statistical significance level was set at $P < 0.05$.

RESULTS

Of 252 patients initially enrolled for the study (mean age 66 years, 67 symptomatic), shoulder PET-CT data were obtained in 200 patients (52 were excluded due to exclusion criteria above). The most common cancer types were lymphoma (n = 61), lung (n = 54) and breast (n = 53). No significant difference was noted between symptomatic and asymptomatic patients in terms of age, gender, proportion of patients who had surgical therapy and radiation therapy. A proportion of patients who received chemotherapy was higher in patients who were asymptomatic in the right shoulder compared to those symptomatic in the right shoulder (65% *vs* 48%, P = 0.012). No such difference was seen for the left shoulder. In both shoulders, SUVmax and SUVmean were higher in symptomatic shoulders than asymptomatic shoulders (Left SUVmax 2.0 *vs* 1.6, SUVmean 1.6 *vs* 1.3, both $P < 0.002$; Right SUVmax 2.2 *vs* 1.8, SUVmean 1.8 *vs* 1.5, both $P < 0.01$). For lung cancer patients, bilateral RI SUVmax and SUVmean values were higher in symptomatic shoulders than asymptomatic shoulders. For other cancer patients, symptomatic patients had higher left RI SUVmax/mean than asymptomatic patients after adjustment.

CONCLUSION

In symptomatic patients metabolic activities in RI were higher than asymptomatic patients. Adhesive capsulitis should be considered in cancer patients with shoulder symptoms and positive FDG uptake in RI.

Key Words: Adhesive capsulitis; Positron emission tomography - computed tomography; Cancer; Shoulder; Pain; Imaging

Core Tip: Adhesive capsulitis is a relatively common condition that can develop in cancer patients during treatment. However, there has been relatively scant literature evidence on Positron emission tomography - computed tomography (PET-CT) findings specific to adhesive capsulitis. Our study showed that, in symptomatic cancer patients, metabolic activities in the rotator interval were higher than asymptomatic patients overall, and also specifically for lung cancer patients. Presence of adhesive capsulitis may explain shoulder pain or stiffness in cancer patients, which can be incidentally diagnosed on PET-CT. Demographic characteristics, treatment regimen, and cancer type did not appear to be an independent risk factor.

Citation: Hayashi D, Gould E, Shroyer R, van Staalduinen E, Yang J, Mufti M, Huang M. Shoulder adhesive capsulitis in cancer patients undergoing positron emission tomography - computed tomography and the association with shoulder pain. *World J Radiol* 2021; 13(10): 344-353
URL: https://www.wjgnet.com/1949-8470/full/v13/i10/344.htm
DOI: https://dx.doi.org/10.4329/wjr.v13.i10.344

INTRODUCTION

Adhesive capsulitis is a relatively common and potentially debilitating disorder of the shoulder joint, with most common onset in the 5th to 6th decades. Typical clinical presentation include shoulder pain, stiffness, and loss of range of motion, and can persist for extended periods of time if not adequately addressed clinically[1-4]. While adhesive capsulitis is a clinical diagnosis, magnetic resonance imaging (MRI) is

Article in press: September 14, 2021
Published online: October 28, 2021

P-Reviewer: Dikaios N
S-Editor: Wang LL
L-Editor: A
P-Editor: Liu JH

currently the most commonly used imaging tool for its diagnosis[5-7], however not all cancer patients undergo MRI of the shoulder unless there is specific clinical suspicion for adhesive capsulitis or other shoulder-specific pathology. Positron emission tomography - computed tomography (PET-CT) is a useful imaging modality for cancer diagnosis, particularly for the purpose of staging and follow-up of malignancy. PET-CT is also useful in monitoring inflammatory disorders, and the shoulder joint can be hypermetabolic on PET-CT when there is active inflammation such as osteoarthritis, inflammatory and infectious arthritis, bursitis, rotator cuff injury, and adhesive capsulitis[8,9]. However, there has been relatively scant literature evidence on PET-CT findings specific to adhesive capsulitis. One study demonstrated radiotracer uptake in the joint capsule of the glenohumeral joint connecting the rotator interval, anterior joint capsule, and axillary recess is related to adhesive capsulitis[10]. Another study found secondary adhesive capsulitis (depicted by PET-CT) after modified radical mastectomy for breast cancer was common (9.6%) and differed in severity and the progression pattern depending on whether the range of motion in the shoulder was mildly or severely limited[11]. Given the fact that PET-CT imaging is routinely performed as a follow-up study in cancer patients after therapy, being aware of PET-CT findings to suggest shoulder adhesive capsulitis may help to alert clinicians for the diagnosis of unsuspected shoulder capsulitis and avoid potential misdiagnosis of cancer progression, while simultaneously allowing for earlier initiation of appropriate therapy of capsulitis to potentially improve outcomes. Therefore, the aims of our study were to: (1) Evaluate the frequency of shoulder capsulitis in cancer patients undergoing PET-CT; (2) Determine if there is correlation between cancer type/ treatment regimen and frequency of adhesive capsulitis; and (3) Evaluate if metabolic activities in the rotator interval (RI) are different between symptomatic and asymptomatic patients.

MATERIALS AND METHODS

Data collection

Our prospective study received Institutional Review Board approval at our institution (Protocol# 2015-3396-R2). Written informed consent was obtained from all patients. All participants (cancer patients) answered a questionnaire regarding shoulder pain or stiffness and its duration at the time of presentation to an imaging study at our institution (outpatient cancer center) between March 2015 and April 2019. Questions included: Do you have shoulder pain or stiffness (yes/no, if yes, which side); if yes, how long have you had shoulder pain? Have you noticed decreased range of motion in the affected shoulder (yes/no)? Is the symptom worse at any particular time of day? Do you have difficulty raising arms above your head or moving your arms behind back (yes/no)? Electronic medical chart review was performed to collect demographic information (age and gender) as well as details of cancer type and treatment regimen (type and date of surgery, type and date/duration of chemotherapy, and type and date/duration of radiation therapy). All eligible cancer patients who presented to our outpatient imaging center for PET-CT imaging within the recruitment period and were willing to participate in the study were included in our study. Patients with advanced glenohumeral arthrosis, metastatic disease or other mass lesion in the shoulder (all of which could give positive FDG uptake without adhesive capsulitis), or history of shoulder arthroplasty were excluded.

PET-CT image acquisition and interpretation

All patients fasted for at least 6 hours prior to the PET-CT scan. Blood glucose levels were measured before the injection of 18F-fluorodeoxyglucose (FDG) and were lower than 200 mg/dL in all patients. PET-CT was performed using a Siemens Biograph LSO (Siemens Healthineers, Erlangen, Germany). Whole-body CT from the basal skull to the thigh was performed with a continuous spiral technique on a 40-slice helical CT scanner (120 kV; 65 mAs, slice thickness of 4 mm) in the supine position with the arms down. Next, an emission scan was performed from head to thigh at 3 min per frame at 60 min after the intravenous injection of 0.14 mCi/kg of 18F-FDG. CT data were used for attenuation correction and PET images were reconstructed with a three-dimensional (3D) ordered-subsets expectation maximization algorithm (20 subsets, two iterations). CT and PET scan data were accurately coregistered on a dedicated workstation.

We evaluated the intensity of 18F-FDG accumulation as standardized uptake values (SUVs), defined as the tissue concentration divided by the activity injected per body weight. A region of interest was drawn in transaxial images showing FDG uptake within the RI and also low grade FDG uptake at the deltoid muscle. SUVs were measured at the RI and the deltoid muscle from attenuation-corrected axial images. Maximum SUV (SUVmax) at a pixel with the highest uptake of 18F-FDG within each region of interest (ROI) as well as the mean SUV (SUVmean) of each ROI were recorded in bilateral shoulders. Normalized SUV (SUV of RI/SUV of deltoid muscle) was also calculated. None of the ROIs included osseous structures or muscles other than deltoid to exclude the effect of the tracer uptake at the bone marrow and other muscles.

Patterns of shoulder capsule 18F-FDG uptake were recorded on PET-CT scan by two experienced board-certified musculoskeletal radiologists and a Musculoskeletal Radiology Fellow, blinded to clinical information. FDG uptake was considered positive and suggestive of adhesive capsulitis if there was hypermetabolism corresponding to the location of RI on fused PET-CT images.

Statistical analyses

Statistical analyses were performed using SAS9.4 (SAS Institute Inc., Cary, NC) to assess if SUV values are different between patients with and without symptoms in both shoulders. Covariates were age, gender, history of therapy (surgery, chemotherapy, and radiation). Wilcoxon rank sum tests were used to compare unadjusted marginal differences for age, SUV measurements between patients with and without shoulder symptoms. Multiple linear regression models were used to examine the relationship between right or left shoulder SUV measurements and symptom status, after adjusting for cancer type, therapy status, gender and age. To enable meaningful statistical analyses, cancer types were classified into the following 5 categories; Breast, lung, lymphoma, "multiple" (= patients who had two or more cancers), and "other" (= includes the rest of patients with only one cancer that is other than breast cancer, lung cancer or lymphoma). Interaction of shoulder symptom status and cancer type was also included in the models to model the differences within each specific cancer types. Statistical significance level was set at $P < 0.05$.

RESULTS

252 patients were initially enrolled (143 women, 109 men, mean age 66 years, 67 symptomatic). Of these, two patients had right sided shoulder arthroplasty and one patient had left sided shoulder arthroplasty, and these affected shoulders were excluded from analyses. One patient had a large mass in the left proximal humerus, and was also excluded from analysis. Other patients who did not have PET-CT imaging of shoulders (*e.g.*, patients who had brain PET-CT only, or bilateral shoulders being outside the field of view) or other applicable exclusion criteria described earlier were also excluded. In the end, there were 200 right shoulder PET-CT imaging, and 200 Left shoulder PET-CT imaging. Most common cancer types were lymphoma (n = 61), lung (n = 54) and breast (n = 53) (Table 1). No statistically significant difference was noted between symptomatic and asymptomatic patients in terms of age, gender, proportion of patients who had surgical therapy and radiation therapy. A proportion of patients who received chemotherapy was higher in patients who were asymptomatic in the right shoulder compared to those symptomatic in the right shoulder (65% *vs* 48%, $P = 0.012$). No such difference was seen for the left shoulder.

In both shoulders, SUVmax and SUVmean were higher in symptomatic shoulders than asymptomatic shoulders (Left SUVmax 2.0 *vs* 1.6, SUVmean 1.6 *vs* 1.3, both $P < 0.002$; Right SUVmax 2.2 *vs* 1.8, SUVmean 1.8 *vs* 1.5, both $P < 0.01$), as shown in Table 2. Based on the multiple linear regression models, for lung cancer patients, bilateral RI SUVmax and SUVmean values were higher in symptomatic shoulders than asymptomatic shoulders after adjustment (Table 3). Examples of symptomatic shoulders with abnormal capsular FDG uptake are shown in Figures 1 and 2. For other cancer patients, symptomatic patients had higher left rotator interval SUVmax and SUVmean than asymptomatic patients after adjustment.

Table 1 The total number and types of cancers that were included in our patient population

Type of cancer	Total number
Lymphoma	61
Lung	54
Breast	53
Head and neck	12
Thyroid	10
Colon	9
Melanoma	9
Multiple myeloma	9
Endometrial	6
Pancreas	5
Bladder	5
Prostate	4
Kidney	3
Sarcoma	3
Esophageal	3
Other[1]	24

[1]"Other" cancers were cases in which the primary tumor type was not yet determined, but the patient already had metastatic disease, or cancer types which had only 2 or fewer patients including stomach, Castleman's disease, bone, cervical, ovarian, neurofibromatosis type 1 small bowel mass, brain, carcinoid, cholangiocarcinoma, small cell carcinoma, penile, anal, Merckel cell, cardiac, tracheal, and rectal cancers.

Table 2 Standard uptake value measurements of right and left shoulders in symptomatic and asymptomatic patients

Left shoulder	**Total (n = 200)**	**Asymptomatic (n = 143)**	**Symptomatic (n = 57)**	***P* value**
RI SUVmax	1.7 ± 0.9	1.6 ± 0.7	2.0 ± 1.1	< 0.001
RI SUVmean	1.4 ± 0.7	1.3 ± 0.6	1.6 ± 0.9	0.002
Deltoid SUVmax	0.9 ± 0.3	0.9 ± 0.3	1.0 ± 0.3	0.068
Deltoid SUVmean	0.8 ± 0.3	0.8 ± 0.3	0.8 ± 0.3	0.281
Normalized SUVmax	1.9 ± 1.3	1.9 ± 1.0	2.0 ± 1.5	0.125
Normalized SUVmean	1.8 ± 1.2	1.8 ± 1.1	1.9 ± 1.6	0.112
Right shoulder	**Total (n = 200)**	**Asymptomatic (n = 143)**	**Symptomatic (n = 57)**	***P* value**
RI SUVmax	1.9 ± 0.8	1.8 ± 0.8	2.2 ± 0.7	0.002
RI SUVmean	1.5 ± 0.7	1.5 ± 0.7	1.8 ± 0.8	0.012
Deltoid SUVmax	0.9 ± 0.3	0.9 ± 0.3	0.9 ± 0.3	0.279
Deltoid SUVmean	0.7 ± 0.2	0.7 ± 0.2	0.8 ± 0.3	0.160
Normalized SUVmax	2.2 ± 1.1	2.2 ± 1.1	2.3 ± 1.5	0.105
Normalized SUVmean	2.1 ± 1.0	2.2 ± 1.0	2.1 ± 1.1	0.392

P value was calculated using Wilcoxon rank sum test and median with Inter Quartile Ratio were reported. These results were unadjusted comparisons. RI: Rotator interval; SUV: Standard uptake value.

DISCUSSION

Adhesive capsulitis is a relatively common condition that can develop and perhaps, can predate, diagnosis of cancer in patients undergoing treatment[12], and can be

Table 3 Multiple linear regression analyses showing association between right or left shoulder standard uptake value measurements and symptom status after adjusting for covariates, stratified by cancer type

Cancer type	Left RI SUVmax		Right RI SUVmax	
	Value	95%CI	Value	95%CI
Breast	0.36	-0.37, 0.44	0.13	-0.51, 0.54
Lung	0.65	0.24, 1.07	0.56	0.14, 0.97
Lymphoma	0.28	-0.14, 0.70	0.08	-0.34, 0.51
Multiple	0.25	-0.21, 0.71	0.23	-0.01, 1.12
Other	0.57	0.23, 0.91	0.22	-0.21, 0.65
Cancer type	**Left RI SUVmean**		**Right RI SUVmean**	
	Value	**95%CI**	**Value**	**95%CI**
Breast	0.05	-0.30, 0.39	-0.03	-0.46, 0.41
Lung	0.50	0.14, 0.86	0.45	0.11, 0.80
Lymphoma	0.19	-0.17, 0.55	-0.06	-0.42, 0.29
Multiple	0.19	-0.21, 0.58	0.45	-0.02, 0.92
Other	0.44	0.14, 0.73	0.28	-0.08, 0.64

There was no statistically significant results for deltoid SUV measurements and normalized SUV measurements for right and left shoulders (results not shown). RI: Rotator interval; SUV: Standard uptake value.

incidentally identified on PET-CT imaging, or other imaging such as ultrasound and MRI[13]. In symptomatic patients, metabolic activities in the RI were higher than asymptomatic patients. The presence of adhesive capsulitis may explain shoulder pain or stiffness in cancer patients, which can be incidentally diagnosed on PET-CT. In general population, it has been shown that risk factors for adhesive capsulitis include age 40 years or older, female gender, immobility or reduced mobility of the shoulder (due to pathologies such as stroke, fracture, recovery from surgery, and rotator cuff injury), and underlying systemic diseases such as diabetes, thyroid disorders, and Parkinson’s disease[14]. In our study sample, demographic characteristics, treatment regimen, and cancer type did not appear to be an independent risk factor.

Diagnostic utility of PET-CT for diagnosis of adhesive capsulitis of the shoulder has been infrequently documented in the literature, some are related to cancer patients[11,14,15] but others are not[10,16,17]. A retrospective analysis of patients with clinically diagnosed adhesive capsulitis showed increased FDG uptake in the RI or inferior glenohumeral joint capsule conferred a moderate increase in the likelihood of adhesive capsulitis[16]. In this study, of the 123 patients, 9 patients had clinical diagnosis of adhesive capsulitis, while 15 patients had FDG uptake in the RI or inferior joint capsule, with the sensitivity and specificity of PET for detection of capsulitis being 56% and 87%, respectively. PET-CT had a positive likelihood ratio for adhesive capsulitis was 6.3 (95%CI: 2.8-14.6)[16].

In a prospective study with 35 middle aged patients with unilateral idiopathic shoulder adhesive capsulitis, correlation between FDG PET-CT depicted metabolic pattern at the four ROIs (RI, anterior joint capsule, axillary recess, and posterior joint capsule) and clinical parameters (pain, functional scores, and passive range of motion) was evaluated[17]. Mean SUVmax values for the four ROIs of the affected shoulder were significantly higher than those of the unaffected shoulder. More specifically, the anterior-inferior capsular portion, including RI and axillary recess, was found to be the main pathologic site of idiopathic adhesive capsulitis and revealed significant correlations between the limited range of motion (both elevational and rotational) and increased FDG uptake in these locations[17].

While the above two studies did show PET-CT can be useful for imaging diagnosis of adhesive capsulitis, they were not directly related to cancer patients, which are actually the primary research interest in our study. A retrospective study including 230 breast cancer patients demonstrated FDG-PET is useful in evaluating adhesive capsulitis after breast cancer treatment[11]. Twenty two patients had clinically identified adhesive capsulitis and were categorized into 2 groups: With severely limited and mildly limited range of motion in the shoulder joint. SUVs of the shoulder

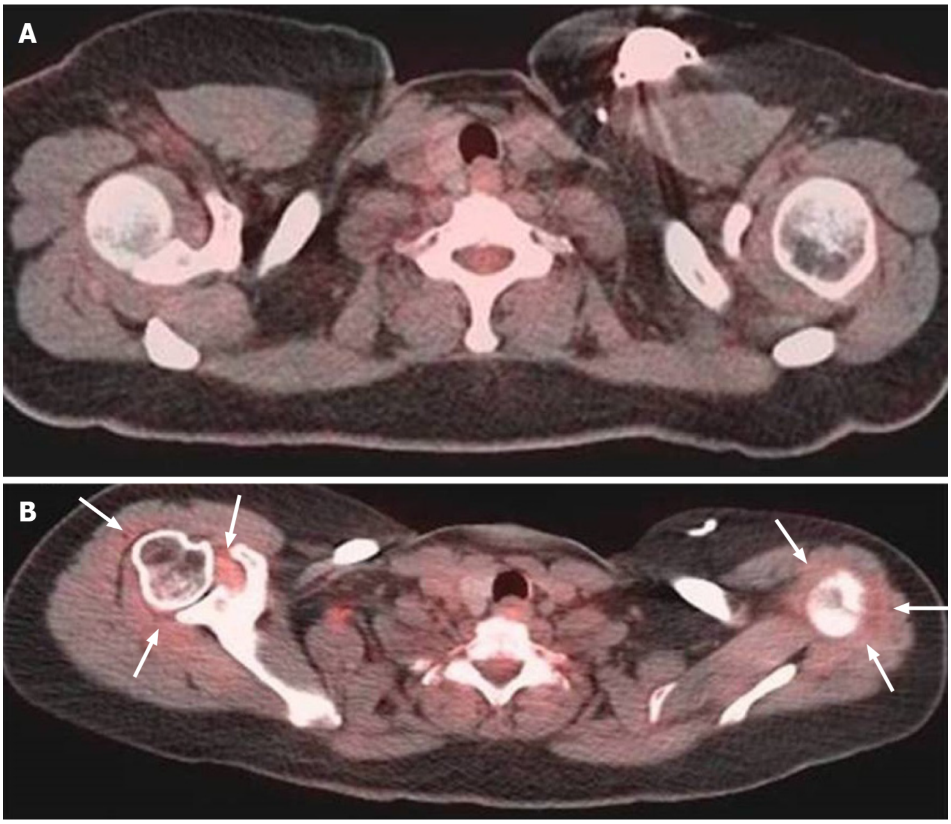

Figure 1 Fifty-two years old patient with lung cancer. A: Initial pre-therapy Positron emission tomography - computed tomography showed no significant capsular 18F-fluorodeoxyglucose (FDG) uptake; B: After the patient was treated with chemotherapy for his lung cancer, the patient developed bilateral shoulder pain with bilateral capsular FDG uptake.

joint capsule were significantly higher in patients with severely limited range of motion compared with those with mildly limited range of motion[11].

Although potentially useful for detection of adhesive capsulitis of the shoulder, interpretation of FDG PET-CT requires caution because a focus of increased metabolic activity can mimic a metastatic lesion in lung cancer patients due to non-specific nature of the positive PET finding and limited anatomical resolution of PET itself as well as potential misregistration of FDG avid focus onto CT images at the time of PET-CT fusion[15]. This is an important point to note, as our study showed the lung cancer was associated with higher SUVs in symptomatic shoulders bilaterally. It is thus important to confirm a suspicion for adhesive capsulitis (raised by PET-CT finding) by dedicated MRI of the shoulder, so as not to mistakenly diagnose a metastasis and potentially altering staging of the cancer and thus management plan.

Interestingly, one large scale study including prospectively collected 2572 incident cancers among 29098 adhesive capsulitis patients showed adhesive capsulitis might be an early predictor for a subsequent cancer[14]. Investigators followed these patients for development of cancer, and found 6-month cumulative incidence of any cancer was 0.70% (standardized incidence ratio [SIR] of 1.38, 95%CI: 1.19-1.58), and risk increases were highest for lung cancer (SIR: 2.19, 95%CI: 1.48-3.13). The findings of our study are in line with this study, in that lung cancer was the only cancer type that showed statistically significant association of higher SUV in symptomatic shoulders. It is unknown why such association was not demonstrated in other types of cancers, despite the fact that there were similar numbers of lymphoma and breast cancer patients in our study. All other types of cancers were likely too small in number to be able to show statistically meaningful association.

Although we attempted to correlate development of capsulitis and potential relationship with different therapy options, no statistically significant association of capsulitis with surgical therapy or radiation therapy was demonstrated. In the right shoulder, a higher proportion of asymptomatic patients received chemotherapy compared to symptomatic patients, but the same was not applicable to the left shoulder. This is likely an incidental finding, as the laterality of the capsulitis is unlikely to be affected by chemotherapy which is a systemic therapy and should not localize to one side of the shoulder.

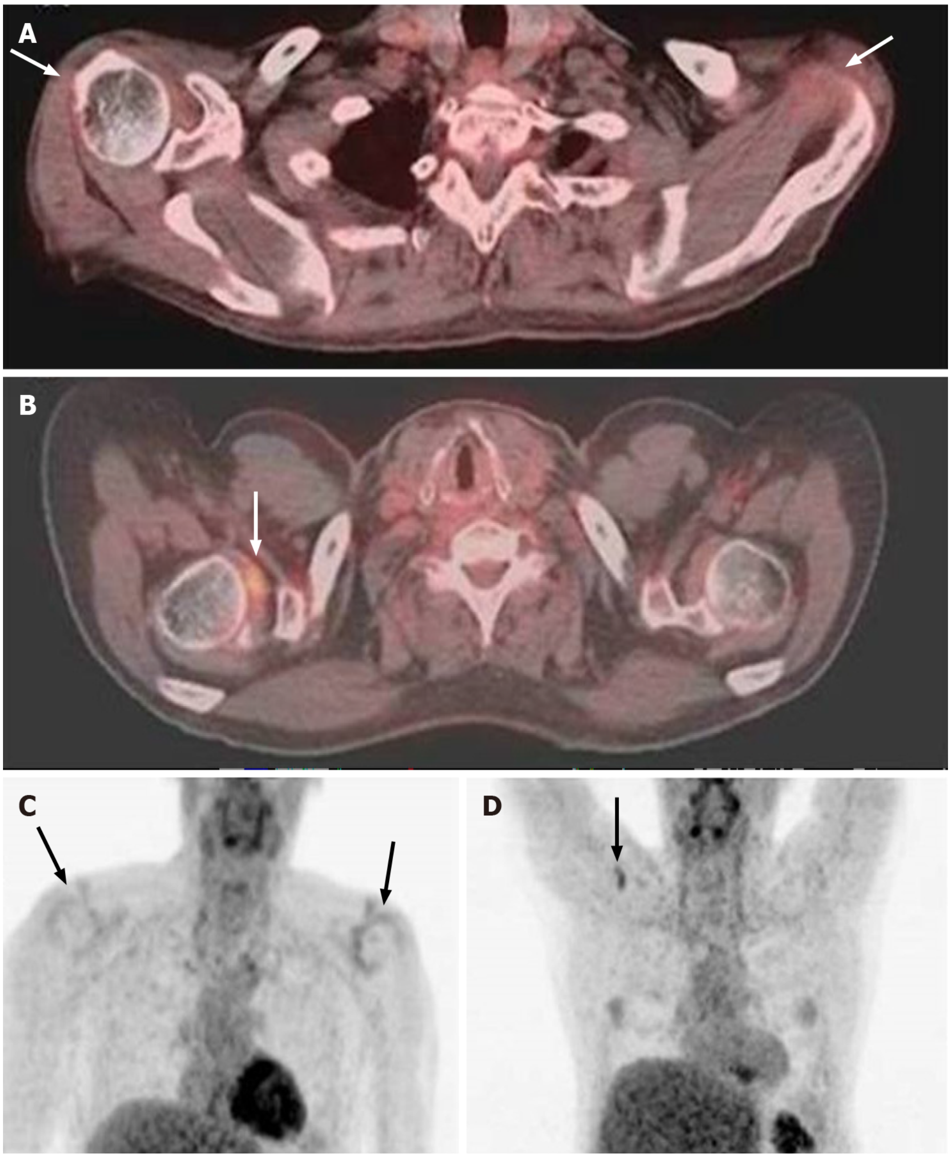

Figure 2 Fifty-six years old patient with lung cancer. Fused Positron emission tomography (PET) - computed tomography (A) and (C) maximum intensity projection (MIP) PET images demonstrate mild diffuse non-specific bilateral shoulder capsular FDG uptake at initial pre-therapy imaging (arrows, better seen on MIP images); B and D: After diagnosis of lung cancer and treatment, the patient developed right shoulder pain and more focal capsular uptake in the right shoulder capsule in the region of rotator interval (arrows).

Limitations of our study include a lack of clinical diagnosis of capsulitis based on clinical examination performed by non-radiologists, and our diagnosis of capsulitis is purely based on PET-CT finding and patient-reported symptoms. We do not know for sure if those patients with positive PET findings actually had clinical exam findings (such as pain and limited range of motion) consistent with adhesive capsulitis. Data collection was performed *via* internal electronic medical record review only. We did not have access to medical records of patients who were managed by physicians outside our institutional network. Lastly, there was no follow-up PET-CT data to assess for resolution of the adhesive capsulitis by imaging.

CONCLUSION

In conclusion, our study showed metabolic activities in RI were higher in symptomatic patients than asymptomatic patients. Although appearance and relationship of capsulitis with malignancy is not fully understood, adhesive capsulitis should be considered in cancer patients with shoulder pain or stiffness and positive FDG uptake in RI, as it may allow for therapy in earlier stages of disease to improve outcomes.

ARTICLE HIGHLIGHTS

Research background

Adhesive capsulitis of the shoulder is a relatively common condition that can develop and possibly predate diagnosis of cancer in patients undergoing treatment. The presence of adhesive capsulitis may explain the presence of shoulder pain or stiffness in cancer patients, which can be incidentally diagnosed on Positron emission tomography - computed tomography (PET-CT).

Research motivation

Since PET-CT imaging is routinely performed as a follow-up study in cancer patients after therapy, being aware of PET-CT findings to suggest shoulder adhesive capsulitis may help to alert clinicians for the diagnosis of unsuspected shoulder capsulitis and avoid potential misdiagnosis of cancer progression.

Research objectives

To: (1) Evaluate the frequency of shoulder capsulitis in cancer patients undergoing PET-CT; (2) Determine if there is correlation between cancer type/treatment regimen and frequency of adhesive capsulitis; (3) Evaluate if metabolic activities in the rotator interval are different between symptomatic and asymptomatic patients. We assessed if Standard Uptake Values (SUVs) are different between symptomatic and asymptomatic patients in both shoulders.

Research methods

In this prospective study, patients answered a questionnaire regarding shoulder pain/stiffness at the time of PET-CT study, between March 2015 and April 2019. Patterns of shoulder capsule 18F-fluorodeoxyglucose (FDG) uptake were noted. SUVmax and SUVmean values were measured at the rotator interval (RI) and deltoid muscle in bilateral shoulders. Wilcoxon rank sum tests were used to compare unadjusted marginal differences for age, SUV measurements between symptomatic and asymptomatic patients. Multiple linear regression models were used to examine the relationship between right or left shoulder SUV measurements and symptom status, after adjusting for covariates.

Research results

200 right shoulders and 200 Left shoulders were included in our study. No significant difference was noted between symptomatic and asymptomatic patients in terms of age, gender, proportion of patients who had surgical therapy and radiation therapy. In both shoulders, SUVmax and SUVmean were higher in symptomatic shoulders than asymptomatic shoulders (Left SUVmax 2.0 *vs* 1.6, SUVmean 1.6 *vs* 1.3, both $P < 0.002$; Right SUVmax 2.2 *vs* 1.8, SUVmean 1.8 *vs* 1.5, both $P < 0.01$). For lung cancer patients, bilateral RI SUVmax and SUVmean values were higher in symptomatic shoulders than asymptomatic shoulders.

Research conclusions

In symptomatic patients metabolic activities in the RI were higher than asymptomatic patients. Adhesive capsulitis should be considered in cancer patients with shoulder pain or stiffness and positive FDG uptake in the RI, as it may allow for therapy in earlier stages of disease to improve outcomes.

Research perspectives

Future studies may endeavor to perform radiomics research (texture analysis) on the PET-CT images.

REFERENCES

1 **Manske RC**, Prohaska D. Diagnosis and management of adhesive capsulitis. *Curr Rev Musculoskelet Med* 2008; **1**: 180-189 [PMID: 19468904 DOI: 10.1007/s12178-008-9031-6]

2 **Neviaser AS**, Hannafin JA. Adhesive capsulitis: a review of current treatment. *Am J Sports Med* 2010; **38**: 2346-2356 [PMID: 20110457 DOI: 10.1177/0363546509348048]

3 **Brue S**, Valentin A, Forssblad M, Werner S, Mikkelsen C, Cerulli G. Idiopathic adhesive capsulitis of the shoulder: a review. *Knee Surg Sports Traumatol Arthrosc* 2007; **15**: 1048-1054 [PMID: 17333122 DOI: 10.1007/s00167-007-0291-2]

4 **Hand GC**, Athanasou NA, Matthews T, Carr AJ. The pathology of frozen shoulder. *J Bone Joint Surg Br* 2007; **89**: 928-932 [PMID: 17673588 DOI: 10.1302/0301-620X.89B7.19097]

5 **Emig EW**, Schweitzer ME, Karasick D, Lubowitz J. Adhesive capsulitis of the shoulder: MR diagnosis. *AJR Am J Roentgenol* 1995; **164**: 1457-1459 [PMID: 7754892 DOI: 10.2214/ajr.164.6.7754892]

6 **Carrillon Y**, Noel E, Fantino O, Perrin-Fayolle O, Tran-Minh VA. Magnetic resonance imaging findings in idiopathic adhesive capsulitis of the shoulder. *Rev Rhum Engl Ed* 1999; **66**: 201-206 [PMID: 10339775]

7 **Yoon JP**, Chung SW, Lee BJ, Kim HS, Yi JH, Lee HJ, Jeong WJ, Moon SG, Oh KS, Yoon ST. Correlations of magnetic resonance imaging findings with clinical symptom severity and prognosis of frozen shoulder. *Knee Surg Sports Traumatol Arthrosc* 2017; **25**: 3242-3250 [PMID: 26611904 DOI: 10.1007/s00167-015-3887-y]

8 **Wandler E**, Kramer EL, Sherman O, Babb J, Scarola J, Rafii M. Diffuse FDG shoulder uptake on PET is associated with clinical findings of osteoarthritis. *AJR Am J Roentgenol* 2005; **185**: 797-803 [PMID: 16120937 DOI: 10.2214/ajr.185.3.01850797]

9 **Glaudemans AW**, de Vries EF, Galli F, Dierckx RA, Slart RH, Signore A. The use of (18)F-FDG-PET/CT for diagnosis and treatment monitoring of inflammatory and infectious diseases. *Clin Dev Immunol* 2013; **2013**: 623036 [PMID: 24027590 DOI: 10.1155/2013/623036]

10 **Kim du H**, Sung DH, Ga HY, Choi JY. Metabolic patterns of the shoulder joint on (18)F-fluorodeoxyglucose positron emission tomography/computed tomography in adhesive capsulitis. *Ann Nucl Med* 2014; **28**: 136-144 [PMID: 24317879 DOI: 10.1007/s12149-013-0794-5]

11 **Park JH**, Lee YK, Kim DH, Kim SJ, Lee JH, Jeon TJ, Ryu YH, Lee JD. Usefulness of 18F-fluorodeoxyglucose Positron Emission Tomography-Computed Tomography in Monitoring Adhesive Capsulitis After Breast Cancer Treatment. *J Comput Assist Tomogr* 2015; **39**: 349-355 [PMID: 25700225 DOI: 10.1097/RCT.0000000000000222]

12 **Yang S**, Park DH, Ahn SH, Kim J, Lee JW, Han JY, Kim DK, Jeon JY, Choi KH, Kim W. Prevalence and risk factors of adhesive capsulitis of the shoulder after breast cancer treatment. *Support Care Cancer* 2017; **25**: 1317-1322 [PMID: 27942856 DOI: 10.1007/s00520-016-3532-4]

13 **Kim JH**, Kim SH, Kim HR, Lee SH, Yoon SY, Yang JH, Yoo YB, Park KS, Nam SE, Hong S, Min HK. Ultrasonographic evaluation of chronic shoulder pain after breast cancer surgery: single center, cross-sectional study. *Sci Rep* 2020; **10**: 16792 [PMID: 33033299 DOI: 10.1038/s41598-020-73769-8]

14 **Pedersen AB**, Horváth-Puhó E, Ehrenstein V, Rørth M, Sørensen HT. Frozen shoulder and risk of cancer: a population-based cohort study. *Br J Cancer* 2017; **117**: 144-147 [PMID: 28524156 DOI: 10.1038/bjc.2017.146]

15 **Salem U**, Zhang L, Jorgensen JL, Kumar R, Amini B. Adhesive capsulitis mimicking metastasis on 18F-FDG-PET/CT. *Clin Nucl Med* 2015; **40**: e145-e147 [PMID: 24999685 DOI: 10.1097/RLU.0000000000000524]

16 **Sridharan R**, Engle MP, Garg N, Wei W, Amini B. Focal uptake at the rotator interval or inferior capsule of shoulder on ^{18}F-FDG PET/CT is associated with adhesive capsulitis. *Skeletal Radiol* 2017; **46**: 533-538 [PMID: 28161721 DOI: 10.1007/s00256-017-2587-8]

17 **Won KS**, Kim DH, Sung DH, Song BI, Kim HW, Song KS, Lee SW, Cho CH. Clinical correlation of metabolic parameters on ^{18}F-FDG PET/CT in idiopathic frozen shoulder. *Ann Nucl Med* 2017; **31**: 211-217 [PMID: 28168397 DOI: 10.1007/s12149-016-1147-y]

Published by **Baishideng Publishing Group Inc**
7041 Koll Center Parkway, Suite 160, Pleasanton, CA 94566, USA
Telephone: +1-925-3991568
E-mail: bpgoffice@wjgnet.com
Help Desk: https://www.f6publishing.com/helpdesk
https://www.wjgnet.com